AN ABSTRACT OF THE THESIS OF

Nicklas George Pisias (Name) for the Master of Science (Degree)

in Oceanography (Major) presented on December 12, 1973 (Date)

Title: MODEL OF LATE PLEISTOCENE-HOLOCENE VARIATIONS IN RATE OF SEDIMENT ACCUMULATION: PANAMA BASIN, EASTERN EQUATORIAL PACIFIC

Abstract approved: Signature redacted for privacy.

G. Ross Heath

Signature redacted for privacy.

Theodore C. Moore, Jr.

The assumption of constant quartz accumulation for the deep-sea sediment core Y69-106P, taken in the Panama Basin, has been used to date the core and construct a sedimentation rate versus time curve for it. Stratigraphic control for the calculated time scale includes three carbon-14 measurements, the extinction of the radiolarian Stylatractus universus, and correlation with oxygen isotope curves from other dated cores.

The model sedimentation rates and sediment composition data allow the determination of sediment accumulation rates for calcium carbonate, opaline silica, and remaining "detritus". Fluctuations in calcium carbonate accumulation rates correlate closely with variations in oxygen isotope ratios in biogenous carbonate from two

other equatorial Pacific sediment cores. High oxygen isotope ratios correlate with high calcium carbonate accumulation rates. Opaline silica accumulation rates reflect changes in the dominance of radiolarian fossil groups which can be related to surface circulation in the Panama Basin. The successive maxima in opal and calcium accumulation rates and the oxygen isotope ratios in Y69-106P suggest that at the end of the last glacial period, the rate of calcium carbonate dissolution increased in the Panama Basin first, to be followed by a decrease in the intensity of the eastern equatorial Pacific upwelling, and finally the volume of continental glaciers decreased.

Spectral analysis of the rate of accumulation of calcium carbonate in Y69-106P and of the oxygen isotope record of core V28-238 indicate the presence of a 23,000 year periodicity. Analysis of opal accumulation rate suggest a 100,000 year periodicity. These two periodicities are found in fluctuations in the earth's orbital parameters. The eccentricity of the orbit fluctuates with an average period of 98,000 years and the precession of the equinoxes changes with a 22,000 year period.

Model of Late Pleistocene-Holocene Variations in Rate of Sediment Accumulation: Panama Basin, Eastern Equatorial Pacific

by

Nicklas George Pisias

A THESIS

submitted to

Oregon State University

in partial fulfillment of
the requirements for the
degree of

Master of Science

June 1974

APPROVED:

Signature redacted for privacy.

Associate Professor in Oceanography
in charge of major

Signature redacted for privacy.

Associate Professor in Oceanography
in charge of major

Signature redacted for privacy.

Dean of the School of Oceanography

Signature redacted for privacy.

Dean of Graduate School

Date thesis is presented December 12, 1973

Typed by Linda Wille for Nicklas George Pisias

ACKNOWLEDGEMENTS

I have been very fortunate to have had Drs. Ted Moore and Ross Heath as my major advisors during this phase of my academic career. Their guidance, patience and encouragement during my work are deeply appreciated. I also wish to acknowledge the other members of my committee, Drs. D. Thomas and A. Pritchard, for their comments and suggestions.

Dr. J. Dymond provided the argon data. Drs. L. Hogan and J. Dymond helped clarify the problems encountered with the radiometric dates. Dr. N. Shackleton provided the oxygen isotope data which greatly enhanced the conclusions of this thesis.

Dr. B. Somayajulu supplied the Thorium-decay measurements. P. Price and C. Rathbun did many of the sediment analyses used in this thesis and provided much assistance in the lab. I sincerely thank them.

Discussions with B. Malfait, M. Dinkelman, R. Kowsmann and Dr. H. Sachs, whose own work greatly helped in the interpretation of my own data, were extremely helpful. L. Ochs and K. Keeling offered assistance with computer programming. I thank Linda Wille for typing the final drafts of the thesis. I especially thank Dave Rea for reading the early drafts of the thesis and deciphering my impenetrable "English".

To my parents, I thank them for their years of patience and trust. Finally, I thank my wife, Susan, for sharing in the ups and downs encountered when writing a thesis, and who always offered encouragement when it was most needed.

This work was supported by the National Science Foundation through the International Decade of Oceanographic Exploration, CLIMAP Project (Grant No. GX-28673A).

TABLE OF CONTENTS

LIST OF TABLES

LIST OF FIGURES

LIST OF FIGURES, continued

MODEL OF LATE PLEISTOCENE-HOLOCENE VARIATIONS IN RATE OF SEDIMENT ACCUMULATION: PANAMA BASIN, EASTERN EQUATORIAL PACIFIC

INTRODUCTION

Object of the Study

One goal of the marine stratigrapher is to reconstruct the history of the earth's climate which is recorded in ocean floor sediments. A deep-sea sediment core represents a detailed record of the ocean's response to various climatic conditions. These records, unlike those obtained from studies of continental deposits, give a relatively continuous history of climatic changes over long periods of time. The detail of the climatic record determined from deep-sea sediments varies with the rate of sediment accumulation. Cores with normal pelagic rates of accumulation (1-3 cm/1000 years) give a picture of climatic change over the last one million years (see Shackleton and Opdyke, 1973) with a detail of no more than one sample per 1000 years. High sedimentation rate cores taken near oceanic margins yield records of climatic change for the past 50,000 years with a sampling detail of less than 200 years (Pisias et al., 1973). The study of very high sedimentation rate cores may give climatic history spanning the entire Holocene epoch and with a record as detailed as those deduced from tree ring studies (see Fritts et al., 1971).

Interpretation of the climatic records preserved in deep-sea sediment cores is dependent on establishing a good time scale for the cores being studied. An accurate time scale is necessary when studying time transgressive events such as the movement of oceanographic fronts, major current systems (McIntyre et al., 1972), or any sequence of changes in oceanic processes that result from climatic change. Statistical analysis of climatic fluctuations, (for example spectral analysis), demands the best possible time scale. Usually a time scale is estimated by dating levels in a core and assuming continuous and constant sedimentation between these age levels. Sediment samples can be dated either directly by radiometric analysis or indirectly by recognition of previously dated paleomagnetic or stratigraphic events. Sedimentation rates can also be estimated from measurements of the activity of radiogenic elements such as thorium-230 and protactinium-231 (Ku, 1966). But again a constant sedimentation rate is usually assumed.

All of these methods give average sedimentation rates for long periods of geologic time, and only if many data points are determined can temporal change in sedimentation rates be observed. Where such changes in sedimentation rates are observed, an abrupt change from one average rate to another is usually assumed. Rarely is a continuously fluctuating sediment accumulation rate given for a deep-sea sediment core.

To overcome the limitation imposed by a finite number of age determinations and to examine the relationship between climate and accumulation rates, a sedimentation rate model has been constructed. The assumption made in this model is that one component of the sediment accumulates at a constant rate. In the absence of adequate radiometric dating, similar models were used by Wiseman (1956) and Arrhenius (1952). Wiseman in his study of equatorial Atlantic cores assumed that deep-sea sediments consisted of only two components, calcium carbonate accumulating at a variable rate and fine grained silicate detritus, accumulating at a constant rate. This assumption of a constant accumulation rate for fine grained silicate detritus in the equatorial Atlantic has subsequently been disproved (Broecker et al., 1958). Arrhenius assumed that fine grained detritus in equatorial Pacific cores accumulated at a constant rate and that TiO_2 concentration could be used as a measure of its abundance. The time scale given by Arrhenius compares well with other equatorial cores dated by paleomagnetic stratigraphy (Hays et al., 1969).

In the sedimentation rate model constructed here a sediment sample is considered to be a combination of four components: calcium carbonate, opaline silica, crystalline quartz, and "detritus". Of these four components it is assumed that the accumulation of quartz is constant. This model requires the measurement of

concentrations of the sedimentary component and bulk density of samples from a core in which there are no hiatuses and a minimal reworking of sediment. For both the calculation of the model and the testing of the accuracy of the model, age determinations of levels in the core are also required.

Core Location

The cores used in this study were taken by the R/V Yaquina of Oregon State University during the YALOC-69 cruise to the Panama Basin. The Panama Basin, located in the eastern equatorial Pacific, is bounded by the land masses of Central and South America to the northeast and east respectively, and by the submerged Carnegie and Cocos Ridges to the south and northwest. The basin is divided into a western and a deeper eastern basin by the Malpelo and Coiba Ridges (Figure 1). The physiography and tectonics of the basin have been described by van Andel et al. (1971). Surface sediment characteristics were studied by Kowsmann (1973), Moore et al. (1973), Heath et al. (1974) and van Andel (1973). The detailed study of accumulation rates of the four sedimentary components already mentioned and of the total sediment for two cores from the Panama Basin, Y69-106P and Y69-73P forms the heart of this study. The locations of the two cores are given in Figure 1 and Table 1. The low sedimentation rate of Y69-106P, about 2cm/1000 years,

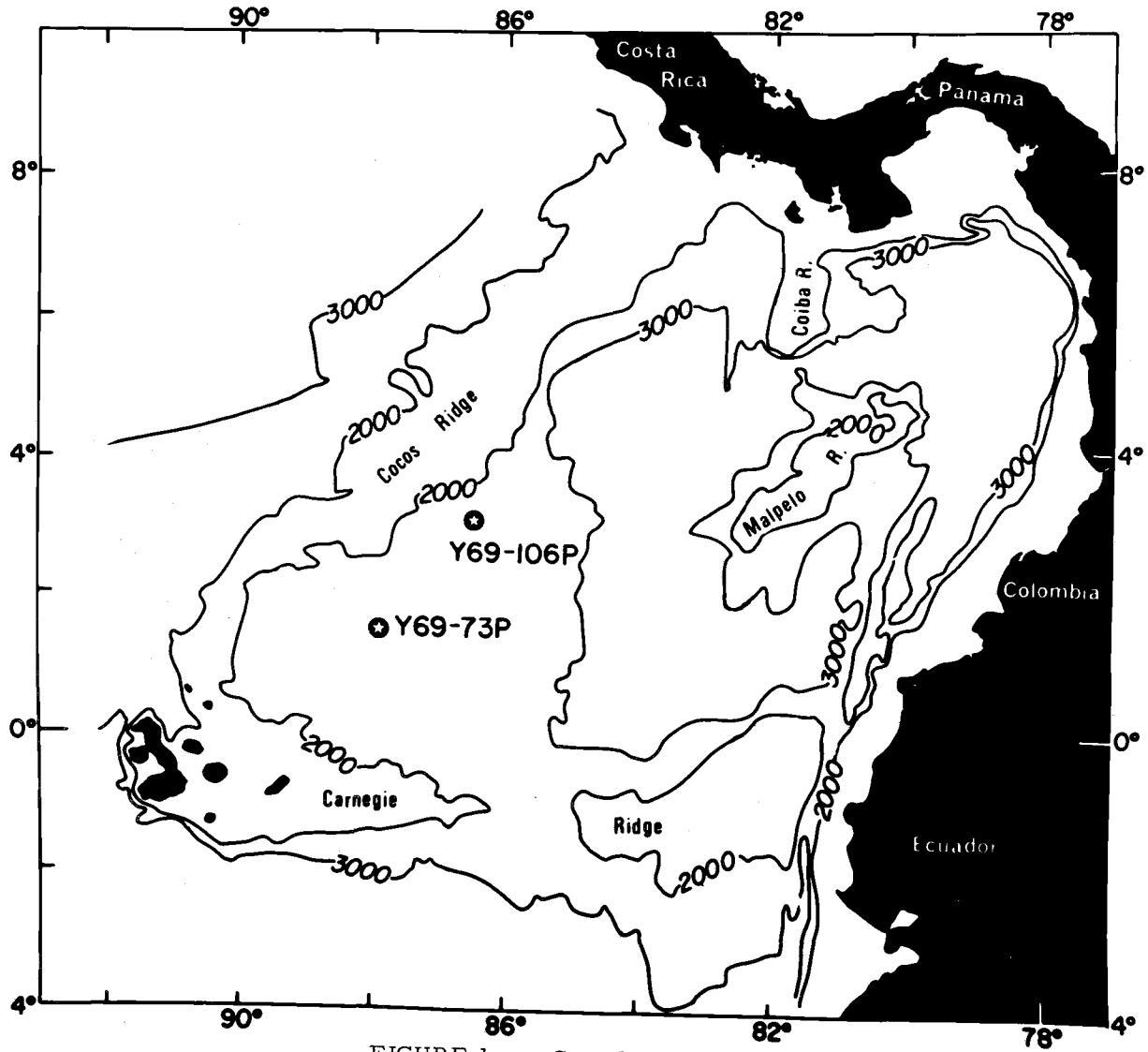

FIGURE 1 Core location map

TABLE 1

Core	Location	Water Depth (m)	Sample Depth (cm)	C^{14} Age (yrs.)	Sedimentation Rates (cm/1000 yrs.)
Y69-106P	2°59'N 86°33'W	2870	0 - 6	4,450 ± 110	
					2.07
			10 - 15	9,030 ± 155	
					1.93
			29 - 36	19,400 ± 800	
Y69-73P	1°27'N 87°56'W	2707	0 - 5	3,590 ± 100	
					9.04
			48 - 53	8,900 ± 150	
					12.65
			165 - 175	18,350 ± 320	

(Table 1) and its length allowed the recovery of sediments deposited during the last three glacial-interglacial cycles. The core was taken just east of the Cocos Ridge where reflection records show stratified sediments that are about .4 kilometers thick (van Andel et al., 1971). From light scattering data, Plank et al. (1973) conclude that there is little erosion of material in the grain size they studied (2-10μm) at this core site. The core consists mostly of pale olive (Munsell code 10Y6/2) foraminiferal clay, with two distinct volcanic ash layers at 120 cm and 506 cm below the top of the core. The mean carbonate content is 65% with increasing carbonate at the base of the core.

Core Y69-73P was taken at a depth approximately 100 m shallower than Y69-106P and in the region of the Galapagos Rift Zone. The sediments in this region are very thin and acoustically semi-transparent (van Andel et al., 1971), and the topography is very irregular. Three carbon-14 dates for this core give sedimentation rates of 9 to 12 cm/1000 years, more than four times the value of Y69-106P. The sediment is a light grayish olive to pale olive brown (10Y5/2 to 5Y5/4) foraminiferal clay. The mean calcium carbonate concentration is 75%, about 10% higher than the mean value for Y69-106P.

Sediment Component Analysis

As mentioned previously, four sedimentary components are considered in this study: calcium carbonate, opaline silica, crystalline quartz, and "detritus". Calcium carbonate was determined using the WR-12 furnace manufactured by the Laboratory Equipment Corporation (LECO). All measured carbon was assumed to be in the form of carbonate. Samples were analyzed in duplicate; if the two values differed by more than one percent at least one additional measurement was made. LECO data were processed by computer to yield the average of all runs, which has been taken as the calcium carbonate concentration of the sample.

Opaline silica and crystalline quartz concentrations were determined by X-ray diffraction (Goldberg, 1958; Calverg, 1966). A detailed discussion of the method used in this study is given by Ellis (1972). In brief, samples were freed of calcium carbonate by treatment with buffered acetic acid, then heated to 1000° C to convert the X-ray amorphous opaline silica to cristobalite, and finally X-rayed using a Norelco X-ray diffraction unit equipped with digital and anlog data acquisition systems. Peak intensities of the cristobalite (101) peak (4.09 Å), internal standard α - alumina (012) peak (3.48 Å), and quartz (101) peak (3.34 Å) were computed by a Canberra digital control and data reduction system. The cristobalite peak, which partly overlaps a feldspar peak, was resolved using a

DuPont analog curve resolver. The abundance of quartz and cristobalite, determined by comparing measured peak intensity ratios to standard curves, were then recalculated to percentages of total sediment. The concentration of "detritus" is the residue after subtracting the concentrations of calcium carbonate, opal, and quartz from 100%.

A total of 101 samples at 10 cm intervals from core Y69-106P and 20 samples at 10 cm intervals from Y69-73P were analyzed (Appendix I). The bulk density of alternate samples was also determined. Bulk density is defined as the weight of the dry sediment divided by its volume prior to drying. This measurement involves extracting from the core a known volume of wet sediment which is then dried and weighed.

In addition to the carbon-14 dates already mentioned, thorium-230 measurements were made on samples from Y69-106P by B. L. K. Somayajulu of the Scripps Institute of Oceanography. Potassium-argon and $argon^{40}/argon^{39}$ age measurements for the volcanic ash layer at 506 cm were made by J. Dymond, and oxygen isotope data for the top of this core was supplied by N. Shackleton.

TIME SCALE FOR CORE Y69-106P

Radiometric Data

The distribution of stratigraphic and radiometric data for core Y69-106P is represented in Figure 2, and a summary of the rates determined from radiometric procedures are given in Table 2. As can be seen from Table 2, the radiometric data give average sedimentation rates for this core ranging from .5 to 6.6 cm/1000 years with no two procedures in agreement.

Stratigraphic Data

The extinction of Stylatractus universus in the Pacific and Indian oceans and the Antarctic region occurred at about 400,000 years B.P. according to Hays (1970). This age is based on interpolation of the extinction level between the sediment surface and the Brunhes-Matuyama paleo-magnetic reversal boundary in eleven cores taken in the North Pacific (Table 3, from Hays and Ninkovitch, 1970). The mean age for the extinction in these cores is 400,000 years with a standard deviation of 20,000 years. Two North Pacific cores, V20-109 and V20-119, were not used in this calculation because of extremely young ages for the extinction level. Such extreme values probably reflect the loss of the sediment core tops during coring operations. For core V20-119, oxygen isotope data support the suggestion that the top of the core may be missing

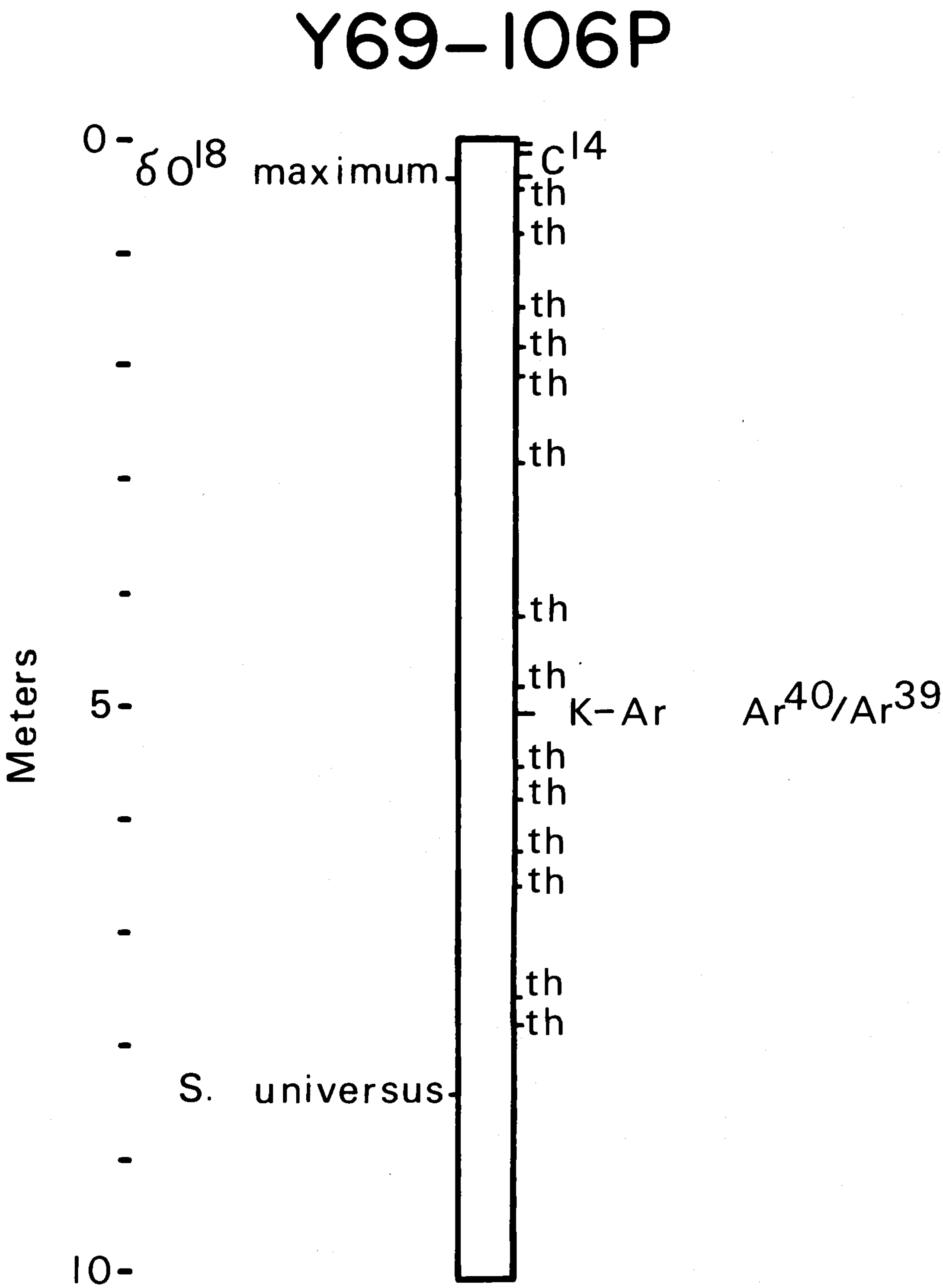

FIGURE 2 Stratigraphic data for time scale of core Y69-106P

TABLE 2

Time scale for core Y69-106P

Method	Samples (cm)	Age (yrs.)	Average Rate (cm/1000 yrs)
		Radiometric	
Carbon-14	0 - 6	4,450 ± 110	2.07
	10 - 15	9,030 ± 155	1.93
	29 - 36	1,940 ± 800	
Potassium-Argon	506	1,000,000 ± 20,000	0.506
Argon-40/Argon-39	506	500,000 ± 10,000	1.0
Thorium-230		(Appendix II)	
		Stratigraphic	
$\delta\ O^{18}$ Maximum	35	17,900 ± 1,300	2.3
S. universus	841	400,000 ± 20,000	2.2
		(Appendix III)	

(Shackleton, written comm.). Since all age estimates of this level could be too young due to a systematic loss of the upper layers of sediment from the piston core, the 400,000 year age is probably a minimum estimate for the age of this stratigraphic level. Four cores taken in the equatorial Pacific (Hays et al., 1969) all give ages younger than 400,000 years (Table 3). This difference in the interpolated age of the extinction of S. universus between the equatorial Pacific and the North Pacific may be real, or again may result from missing core tops in these rather few cores. The four Equatorial cores are more calcareous than the North Pacific cores and if the fluctuation of their calcium carbonate contents indicate varying sedimentation rates, a simple interpolation from the Brunhes-Matuyama paleomagnetic boundary could be systematically in error. If data for all the cores in Table 3 are averaged, with the four smallest values removed, the mean age is 396,000 years. Thus a 400,000 year age for the extinction of S. universus seems to be as good an estimate for this stratigraphic level as can be made at the present time.

Oxygen isotope ratios in the calcareous test of foraminifera reflect the isotope composition of the sea water in which the foraminifera lived and the temperature of deposition. The major control of the isotope ratio of sea water is the amount of ice stored in continental ice masses (Shackleton and Opdyke, 1973). Thus the

TABLE 3

Age of the Extinction of Stylatractus universus

Core	Extinction age
North Pacific Cores	
RC10-167	390,000
V21-145	370,000
V20-119*	335,000
RC10-182	410,000
RC10-181	380,000
V20-109	315,000
V20-108	410,000
V20-107	375,000
RC10-206	390,000
V21-172	440,000
V21-173	410,000
RC11-170	410,000
RC11-171	410,000
Mean	400,000
Equatorial Pacific Cores	
V24-58*	324,000
V24-59*	300,000
V24-60	368,000
V24-62	377,000

Age Histogram

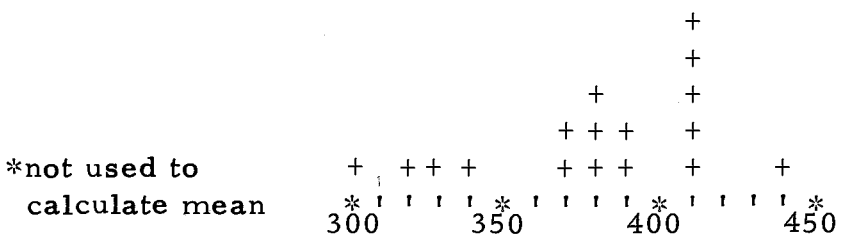

youngest oxygen isotope maximum found in deep-sea sediments represents the last maximum ice advance of the Wisconsin Glacial period. The occurrence of this maximum should be nearly synchronous in all oceans. Any variations in the timing of the event at different localities should be related to the mixing time of the oceans.

Figure 3 shows nine cores for which oxygen isotope analyses have been made. In all cores except V28-238 and P6304-9 carbon-14 measurements are also available. The time scale for core V28-238 is based on the identification of a coccolith datum, the 73,000 year age of which has been determined from cores with carbon-14 dates (Geitzenauer, in press). The time scale for core P6304-9 is taken from Broecker and van Donk (1970) and is based on the identification of "termination II" from the oxygen isotope profiles and an assumed age for this level of 125,000 years. The ages of the youngest oxygen isotope maximum identified in these cores are given in Table 4. The core A180-73 gives an anomalous age, much younger than any of the other cores. When correlated with a neighboring core (A180=74) which has eight carbon-14 ages, core A180-73 consistantly gives younger ages for all stratigraphic datums (Ericson et al., 1961). Therefore, core A180-73 has not been used in the calculation of the mean age of the oxygen isotope maximum. The mean age of this stratigraphic features is 17,900 years with a

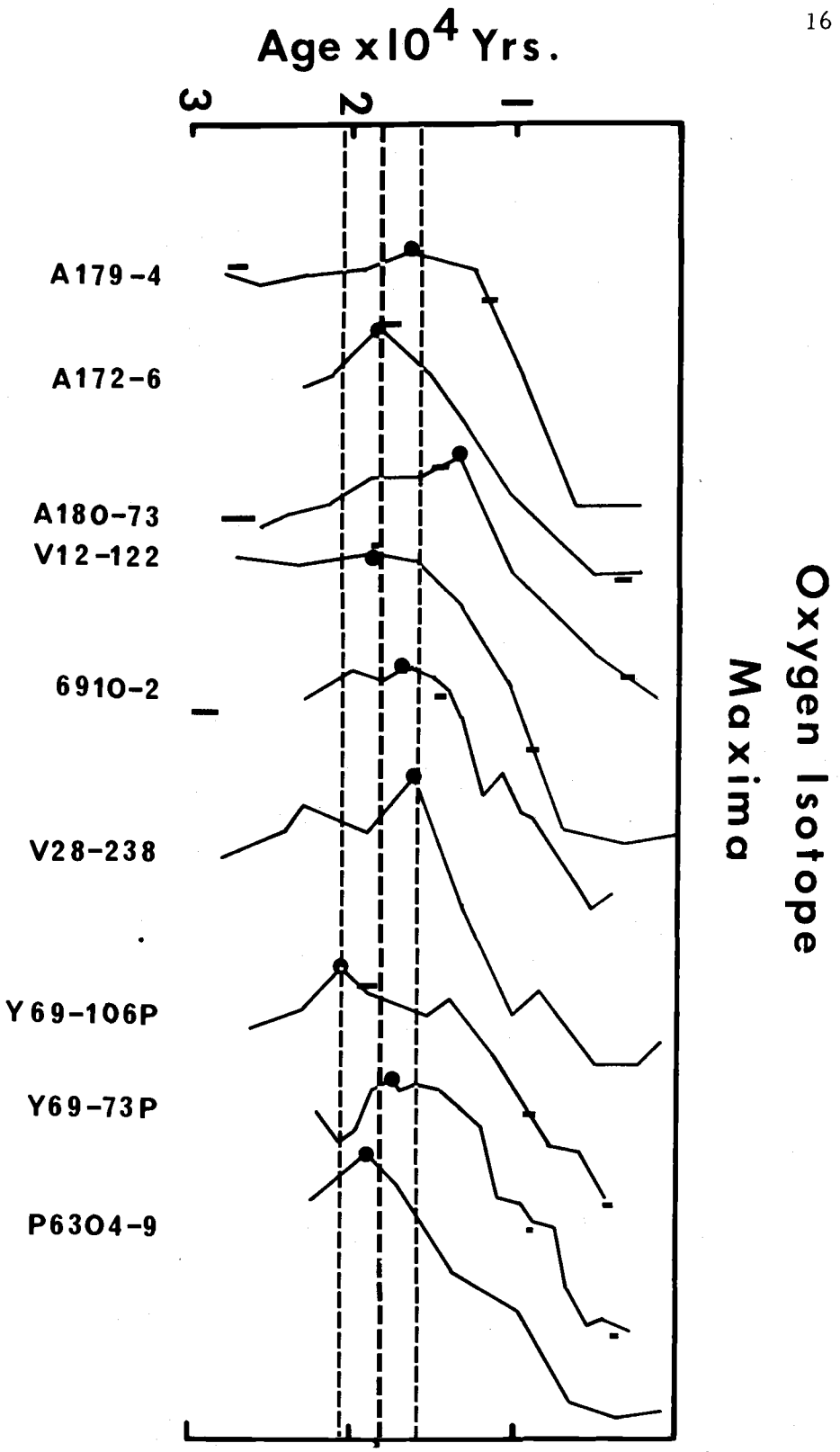

FIGURE 3 Oxygen isotope curves showing youngest oxygen isotope maximum. Boxes on curves indicate carbon-14 dates of cores. Also shown is mean age plus and minus two standard deviations from ages in Table 4.

TABLE 4

Core	Age (yrs.)	Method of Age	Reference
A179-14	16,400	C^{14}	Emiliani, 1955
A172-6	18,400	C^{14}	Emiliani, 1955
A180-73	13,200	C^{14}	Emiliani, 1955
V12-122	18,500	C^{14}	Imbrie and others, 1973
6910-2	16,800	C^{14}	Shackleton, written comm., 1973 Phipps, 1974
V28-238	17,000	bio-stratigraphy dating at 75,000 yrs. (see Table 5)	Shackleton and Opdyke, 1973 McIntyre, written comm., 1973 Geitzernauer, in press
Y69-106P	20,400	C^{14}	Shackleton, written comm., 1973
Y69-73P	17,200	C^{14}	Shackleton, written comm., 1973
P6304-8	18,800	based on the assumption of a 125,000 year age for "termination" II	Broecker and van Donk, 1970
Mean	17,900		

standard deviation of 1300 years. This value is very similar to the age of the last maximum ice advance measured in Europe and North America (G. Denton, written comm., 1973) and the 1300 year standard deviation is of the same magnitude of the mixing time of the oceans.

For core Y69-106P the 400,000 year age of the extinction of S. universus and the 17,900 year age of the youngest oxygen isotope maximum both give an average sedimentation rate of about 2cm/1000 years. This value agrees well with the carbon-14 measurements for the core. The average rate of sedimentation determined from the thorium-230 data is about three times this value; such a discrepancy may result from the relative enrichment of uranium in the sediment of Y69-106P due to reducing conditions of the sediment (Veeh, 1967). No correction was made for the thorium-230 generated by the decay of such an excess. A more complete discussion of the thorium-230 data is given in Appendix II.

Relative to the extinction of S. universus at 841 cm, the potassium-argon age of the volcanic ash at 506 cm is too old to be a depositional age. The extreme age of this sample could be caused by incomplete outgassing of argon during the solidification of the ash. However, the 1,000,000 year date could be the real age of formation of the ash, with its younger stratigraphic position in Y69-106P resulting from subsequent displacement. This latter

explanation is not supported by the restricted stratigraphic distribution of the ash. The argon-40/argon-39 measurements (Brereton, 1970) were made to determine if excess radiogenic argon could be detected and thereby confirm the hypothesis that the 1,000,000 year age is indeed too old because of incomplete outgassing of argon. Unfortunately, the 500,000 year age calculated from the Ar^{40}/Ar^{39} date is suspect because of differing amounts of radiogenic argon measured in the sample by the two techniques (J. Dymond, oral comm., 1973).

MODEL ASSUMPTIONS

Constant Quartz Accumulation

For the sedimentation rate model of Y69-106P it is assumed that the accumulation of quartz has remained constant throughout the late Pleistocene and Holocene epochs. This is consistent with the known pattern of terrigenous sedimentation in the Panama Basin; eolian input is small (Prospero and Bonatti, 1969), and unlikely to vary from glacial to interglacial times; fluviatile input is largely trapped in the eastern basin (Heath et al., 1974); and the deep bottom water circulation responsible for carrying most of the quartz entering the western basin (Heath et al., 1974; Plank et al., 1973) is controlled by geothermal heating (Laird, 1971). The consistency of calculated average rates of quartz accumulation between stratigraphic datums (.0186, .0187, and .0183 grams/cm^2/1000 years for the intervals 0-12, 0-35, 0-341 cm respectively) together with the coherent picture of temporal changes in sedimentation rates produced by the model support the validity of the basic assumption.

Characterization of Data Fluctuations

Additional assumptions which are usually made but not stated in studies of deep-sea sediments and are used in the sedimentation rate model are: a) both the sample interval and the use of linear interpolation between sample points provide an adequate characteri-

zation of the real fluctuations in any parameter of the sediment in a core; b) all maximum and minimum values of a parameter are sampled.

SEDIMENTATION RATE MODEL

Assuming constant quartz accumulation through time, the age at any level in the core is linearly related to the total amount of quartz between that level and the surface of the sediment. The quartz mass curve is calculated from the quartz concentration and the bulk density of the samples in the core. Integration of the quartz mass curve by use of linear interpolation yields a curve of total accumulated quartz mass versus depth in the core. This curve can be converted to age versus depth by calibration using the 400,000 year radiolarian datum, the carbon-14 date at 12.5 cm (9030 years) and the accumulated quartz masses at these levels (Appendix V). The model yields an age at 2 cm depth in the core that is within the error limits of the carbon-14 age for the interval 0 to 6 cm, and gives the age of the oxygen isotope maximum found at 35 cm as 18,400, well within the previously discussed limits for the age of this datum. The calculated average age of the oxygen isotope maximum (Table 4) and the model time scale suggest that the carbon-14 date for the interval 29 to 36 cm is slightly too old. This carbon-14 measurement has a large error associated with it (Table 1).

From the age versus depth relationship determined by the model, sedimentation rates, in cm/1000 years, were calculated for each point. The rate assigned to a sample point is the average of the rates calculated for the intervals preceding and succeeding

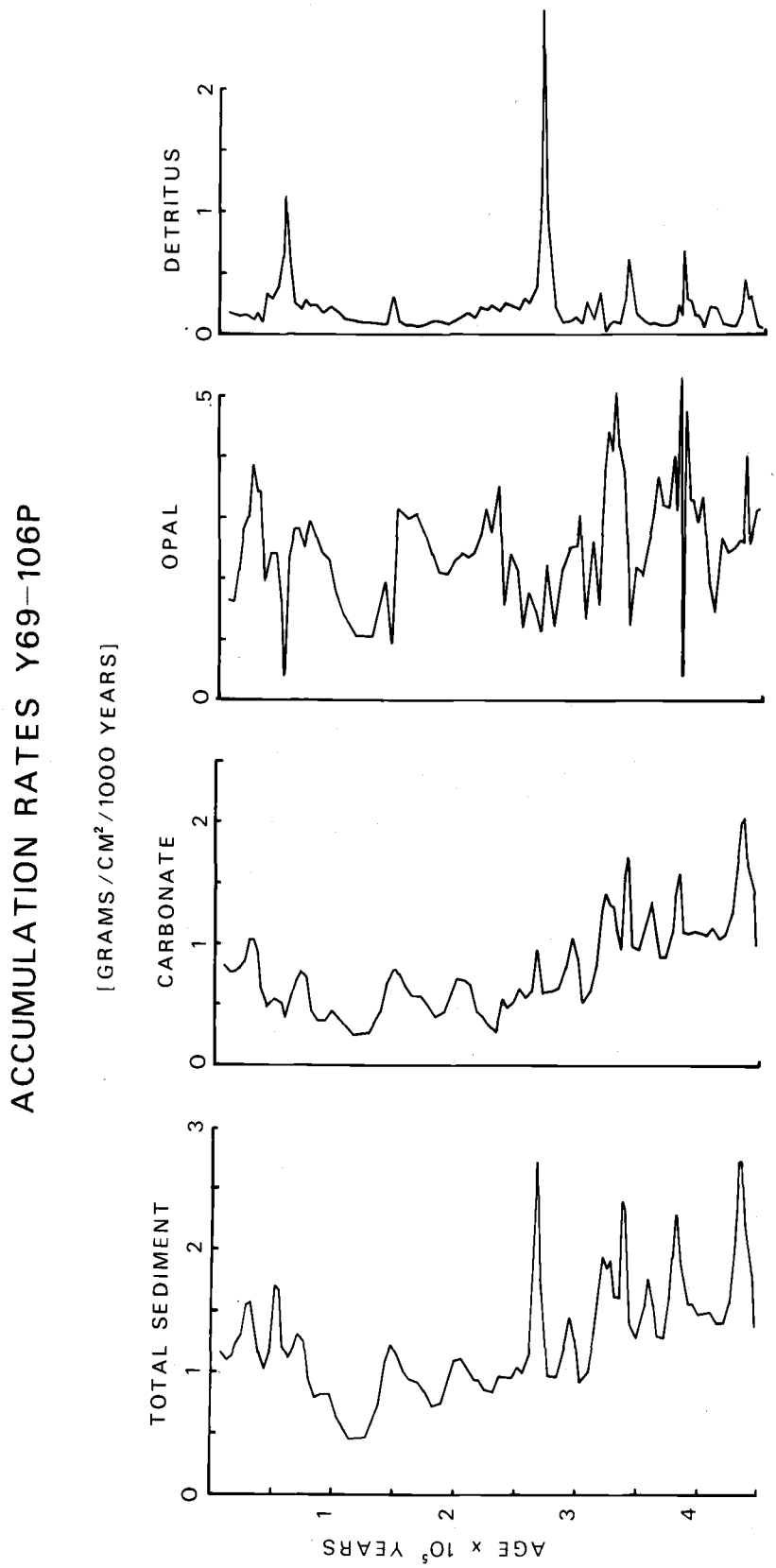

FIGURE 4 Model accumulation rates versus age for core Y69-106P.

each point. The rate of accumulation of individual sediment components is determined from the rate of calculations of the model and the sediment composition data. The accumulation rate of any sedimentary component at a given sample is equal to the product of the total rate of sedimentation (cm/1000 years), the component concentration (weight percent), and the bulk density (gm/cm^3). The rate of each component is expressed in the units gm/cm^2/1000 years. For core Y69-106P the sediment composition data are given in Appendix I. The accumulation rates of calcium carbonate, opaline silica and "detritus" are given in Appendix V and plotted as Figure 4. Results of the sedimentation model calculated for core Y69-73P are given in Appendix IV.

RESULTS AND DISCUSSION OF SEDIMENTATION RATE MODEL - Y69-106P

General

The rate of accumulation of each sedimentary component as a function of age is given in Figure 4. In general there are smooth fluctuations in the sedimentation rates in the younger part of the record, with higher rates and more variation in the samples older than 350,000 model estimated years (e. y.). The "detritus" rates, which clearly show the effect of ash deposition at 51,000 and 267,000 e. y., imply that increased deposition of volcanic ash may have occurred prior to 350,000 e. y. Samples from the lower section of the core also have a higher average calcium carbonate concentration than those from the upper part of the core (75% versus 65%); bulk density values show a similar increase. Clearly, there are indications of an important change in the sedimentation history at this core site at about 350,000 e. y. Either the model is not valid in the lowest section of the core or the intermittent addition of reworked material added a distinct and different signal to the sedimentation record prior to 350,000 e. y. The peaks in the lower section of the "detritus" curve correspond to maxima in the calcium carbonate rate curve and minima in the opaline silica rate (Figure 4). Kowsmann (1973) suggests that foraminiferal sand and volcanic ash are both concentrated by winnowing. This process of reworking

would explain the observed correlation of calcium carbonate with volcanic ash in the oldest part of the sedimentation record in core Y69-106P.

Calcium carbonate and oxygen isotopes

Because of the difficulty in reconstructing temporal changes in sedimentation rates, some very fundamental questions on how climate may affect sedimentation of calcium carbonate and opaline silica are still in debate. Thus, in Atlantic sediments, high carbonate concentrations are correlated with interglacial periods whereas in the Pacific high carbonate concentrations are related to glacial conditions. Wiseman (1954) concluded that the high Atlantic calcium carbonate concentrations during interglacial periods resulted from high productivity due to higher temperatures. However, the assumption of a constant accumulation of detritus used by Wiseman to make this conclusion was shown to be invalid by Broecker et al. (1958). Broecker (1971) later suggested that rates of calcium carbonate accumulation are constant through time in both the Atlantic and Pacific. However, the figure on which Broecker (1971, Figure 9) based his conclusion of constant carbonate sedimentation in the Pacific actually shows 20% higher average carbonate accumulation rates during the last glacial than during the present interglacial period. Arrhenius (1952) hypothesized that

high calcium carbonate concentrations found in sections of equatorial Pacific cores resulted from increased productivity in the surface waters due to more vigorous oceanic circulation during glacial times. Berger (in press) suggests, however, that productivity changes in surface waters of the ocean have a minor effect on carbonate deposition, and that changes in the corrosiveness of bottom waters are the primary control of the accumulation rate of calcium carbonate. The difference in the pattern of accumulation of carbonate between the Pacific and Atlantic is considered by Berger (1970) to reflect the exchange mechanism of surface and bottom waters of the two oceans. At present the Pacific exchanges shallow water for older more corrosive deep waters, resulting in high solution of calcium carbonate in the Pacific Basin. The Atlantic forms its deep water from less corrosive young surface waters and therefore carbonate is more abundant in the Atlantic surface sediments relative to the Pacific. During glacial conditions, the pattern of carbonate distribution in the major ocean is different from the present. In the Pacific, sediment carbonate concentrations are higher during glacial conditions and in the Atlantic, carbonate concentrations were lower. Changes in climate conditions may have affected the exchange processes of surface and deep waters so that during glacial times younger and less corrosive bottom waters entered the Pacific Basin resulting in

improved carbonate preservation.

To help resolve the climatic signal contained in Y69-106P calcium carbonate sedimentation rates are compared with oxygen isotope curves from cores V28-238 taken in the western equatorial Pacific (Shackleton and Opdyke, 1973) (Figure 5). The time scale for core V23-238 was determined by linear interpolation between five known age levels (Table 5). The top of the core was assumed to have a zero age. The sedimentation rate of core V19-55 was about .98 cm/1000 years according to Luz (1973); correlation with the isotope curve of V28-238, however, indicates a slightly lower rate of about .80 cm/1000 years.

The correlation of the carbonate sedimentation rates of Y69-106P with the oxygen isotope curves is very good above the 350,000 year level of the cores, but poor at greater depths (Figure 5). When ice caps were large and sea level low (large δO^{18}) calcium carbonate accumulation rates in the Panama Basin were high, and during high sea level stands and low ice volumes the rates of accumulation were low. This general relationship holds for the past 350,000 years. In detail, however there are some important differences in the timing of the climatic events. Based on ice volume the initial transition from the extreme cold of the Wisconsin glacial period to the present occurred about 17,900 years ago. The

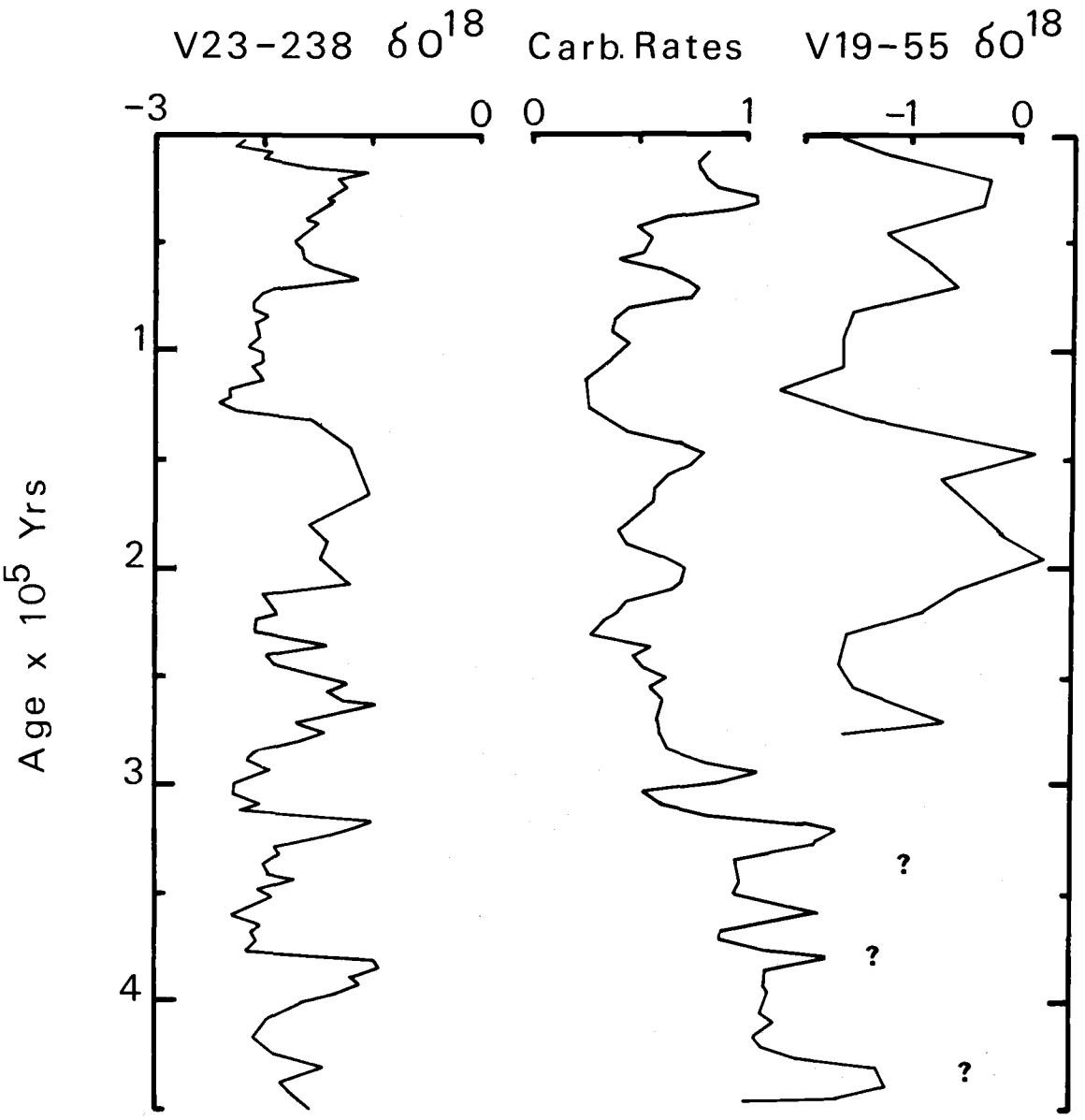

FIGURE 5 Comparison of Y69-106P carbonate rates and oxygen isotope records. Question marks indicate where peaks in carbonate accumulation rate curve believed to be related to reworking have been removed.

TABLE 5

Age Datums of Core V28-238

Datum	Age (yrs.)	Depth in Core (cm)	Sedimentation Rate (cm/1000 yrs.)
Top of core	0 (assumed)	0	
			1.675
δO^{18} Maximum	17,900	30	
			1.9
initial dominance of *E. huxleyi* over *G. caribbeanica*	73,000	135	
			1.5
first appearance of *E. huxleyi*	210,000	335	
			2.6
last occurrance of *S. universus*	400,000	820	
			1.2
Brunhes-Matuyama magnetic boundary	690,000	1200	

Data from: Shackleton and Opdyke (1973)

Geitzenauer (in press)

J. Hays (written comm., 1973)

sedimentation rate model indicates that in the Panama Basin the transition from high sedimentation rates of the last glacial to lower rates of the present interglacial occurred earlier, at 24,000 e. y. The oxygen isotope data for core Y69-106P fixes the point of the last maximum at 35 cm depth in the core (18,400 e. y.). Thus, the minimum lag time between the maximum in the carbonate rate and the δO^{18} maximum is 5,600 years. If the lag time observed is real, the data from Y69-106P provides new insight into climatic changes and its effect on the oceanic system. Although fluctuations in the accumulation of calcium carbonate are well correlated with fluctuations in ice volume, the lag time between these two processes suggests that during climatic change deep water in the Pacific became more corrosive to calcium carbonate, possibly caused by the formation of older bottom waters, prior to changes in ice volume.

Opaline Silica

Opaline silica, like calcium carbonate, is a product of biological activity, and its rate of accumulation in sediments is a function of both the rate of supply of opaline tests from surface waters and the rate of dissolution. The rate of opal solution is highest in relatively warm silica-depleted, near-surface waters

(less than 1000 meters depth); however leaching of silica from deep-sea sediments is an important mechanism in maintaining the geochemical balance of silica in the ocean (Heath, 1974).

Pacific surface sediments in areas of high fertility are characteristically rich in silicous microfossils. But in the Atlantic, surface sediments are relatively silica-poor even in areas of high productivity. The difference in silica preservation between the Atlantic and Pacific reflect differences in the distribution of dissolved silica in the two oceans. The Pacific is enriched in dissolved silica relative to the Atlantic, and therefore is less corrosive to opal. This difference in silica distribution between the major oceans can be explained by the circulation fractionation model discussed by Berger (1970) to describe differences in the deposition patterns of calcium carbonate. The Pacific exchanges surface, silica-depleted water for deep water that is enriched in silica, thus favoring production and preservation of opal. The Atlantic exchanges deep water for shallow water which sinks to form young nutrient-depleted bottom waters which are corrosive to opaline silica.

Because few cores have been analyzed for opal, fluctuations in opaline silica concentrations in equatorial cores have not been related to climatic conditions. The presence of opaline rich sediments in the Pacific beneath highly productive surface waters

suggests that Arrhenius' argument for enhanced deposition due to increased upwelling during glacial times should apply to opal as well as to carbonate concentrations. Again, however, the rate curves of Figure 4 do not allow us to distinguish enhanced producitivy from better preservation.

In order to distinguish the effects of productivity and preservation, it is necessary to examine the faunal and floral makeup of the opaline sediment. For the Panama Basin, Dinkelman (1974) has studied the radiolarian assemblages of surface sediments and related them to productivity and circulation in the surface waters. Using Q-mode factor analysis (Klovan and Imbrie, 1971) of the radiolarian thanatocoenoses, Dinkelman was able to identify four fossil assemblages which he called the "tropical", "solution", "Peru Current", and "equatorial undercurrent" (Cromwell Current) factors.

The two alternative interpretations of these factors given by Dinkelman are: 1) dominance of the "Peru" and "equatorial undercurrent" factors in a sample reflects intensified circulation and upwelling and associated higher productivity due to these currents; or 2) the "Peru" and the "equatorial undercurrent" factors are well preserved fossil groups and the "tropical" and "solution" factors are highly dissolved radiolarian fossil assemblages derived from the same biocoenoses.

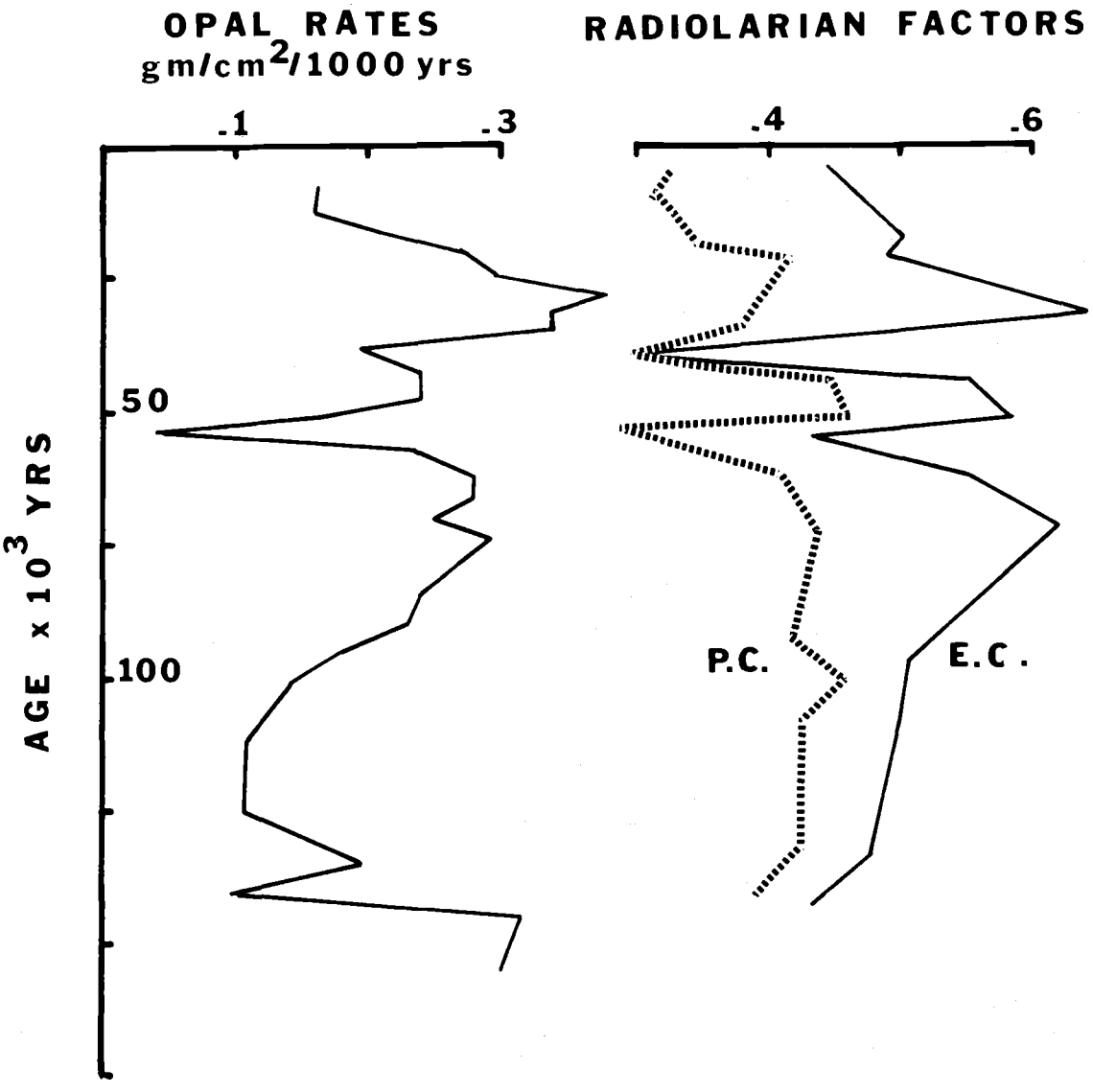

FIGURE 6 Model opal accumulation rates for Y69-106P versus radiolarian fossil assemblage factors. P. C. "Peru Current" factor, E. C. "equatorial undercurrent".

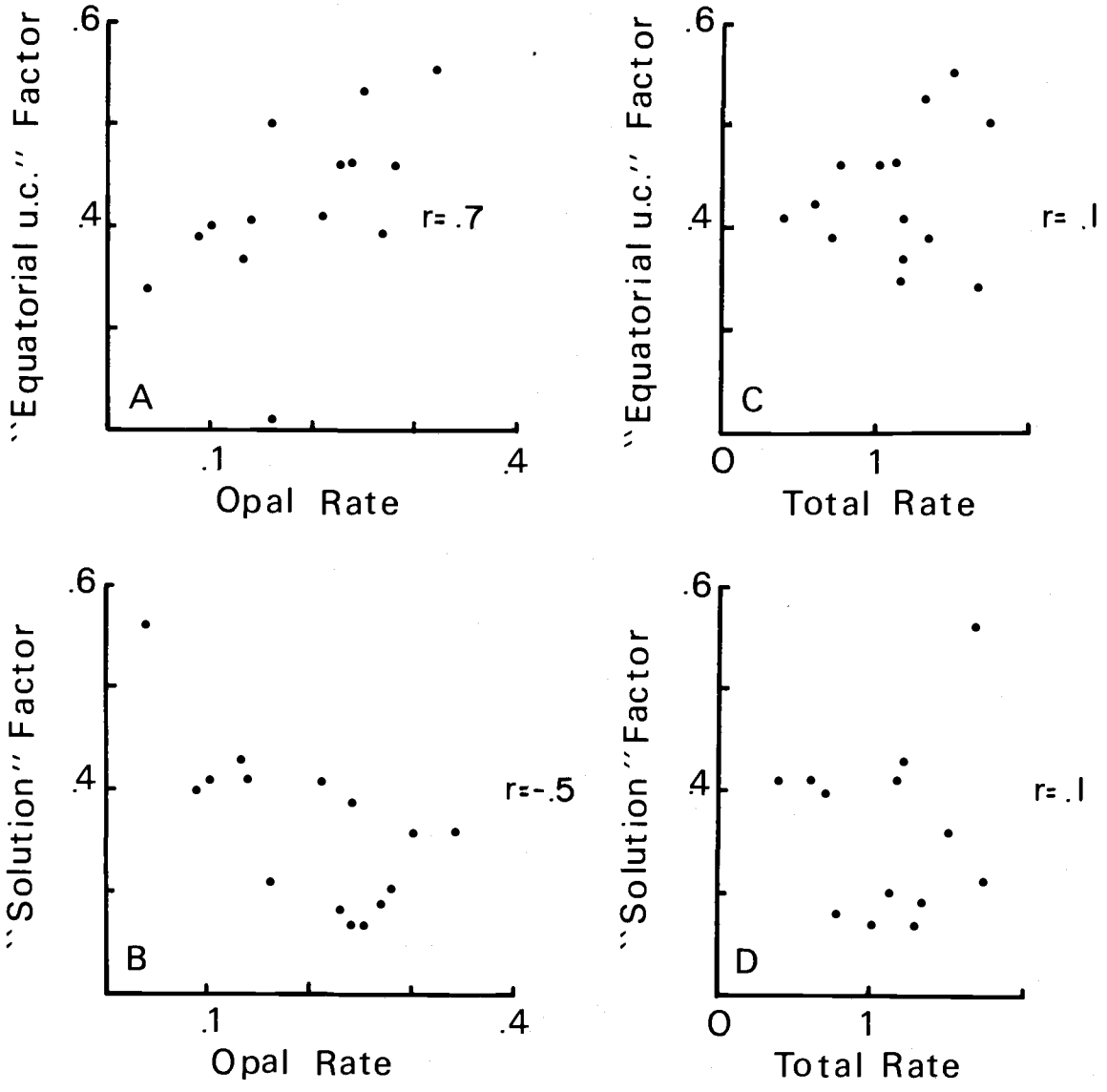

FIGURE 7 Opal and total accumulation rates versus "equatorial undercurrent" and "solution" radiolarian assemblage factors.

By matrix algebra (Imbrie and Kipp, 1971) radiolarian populations in samples from Y69-106P have been resolved into these four radiolarian factors. The relative abundances of the "Peru" and "equatorial" factors for the samples from Y69-106P correlate well with the opal accumulation rates (Figure 6, 7A). Such correlation can be explained by either of Dinkelman's interpretations: minimal solution resulted in high opal accumulation rates and dominant "equatorial" factor, or increased upwelling related to acceleration of the equatorial undercurrent system led to increased rates of supply of opaline silica. If the first explanation is correct, the magnitude of the "solution" factor in the core samples should be negatively related to the total sedimentation rate. This is assuming that the diffusion of silica from deep-sea sediments is restricted to the upper layer (4 cm) of the sediment (Heath, 1974), and that low sedimentation rates increased solution of opaline test due to long exposure to bottom waters. Likewise, if the "equatorial" factor is controlled by solution, its fluctuations should be positively related to fluctuations in the total sedimentation rate. These relationships do not appear to exist in this core. The magnitude of neither the "solution" nor the "equatorial" factors are significantly correlated with the total sedimentation rates of Y69-106P (Figure 7C, 7D).

Thus, the "equatorial" factor shows a positive correlation with opal accumulation but shows no correlation with total sedimenta-

tion rate (Figure 7A, 7C), and the "solution" factor is negatively correlated with the opal accumulation rates and not correlated with total sediment accumulation rates (Figure 7B, 7D). Therefore, for this core either 1) the rate of opal supply is relatively uniform and independent of carbonate supply and dissolution, with variable silica dissolution; or 2) the supply of opal is variable with relatively uniform silica dissolution. At present, the second alternative is considered to apply to core Y69-106P, a conclusion supported by an observational estimate of dissolution in the radiolarian assemblages from this core which show no significant differences between samples (Dinkelman, 1974).

The accumulation rates of opaline silica and calcium carbonate during the last 150,000 years are very similar (Figure 8). However the two curves indicate a slight lag during this time period; the decrease in calcium carbonate at about 60,000 e. y. is succeeded by a decrease in opal rates (Figure 8, d, d'). The last maximum of the calcium carbonate rate curves slightly preceeds the last maximum of the opal rate curve (Figure 8, a, a'). The processes controlling the calcium carbonate and opaline silica accumulation rates seem to be responding to the same changes in the driving mechanism, the climate, but the response times are different. The average lag time between changes in bottom water characteristics (carbonate rates) and changes in surface water

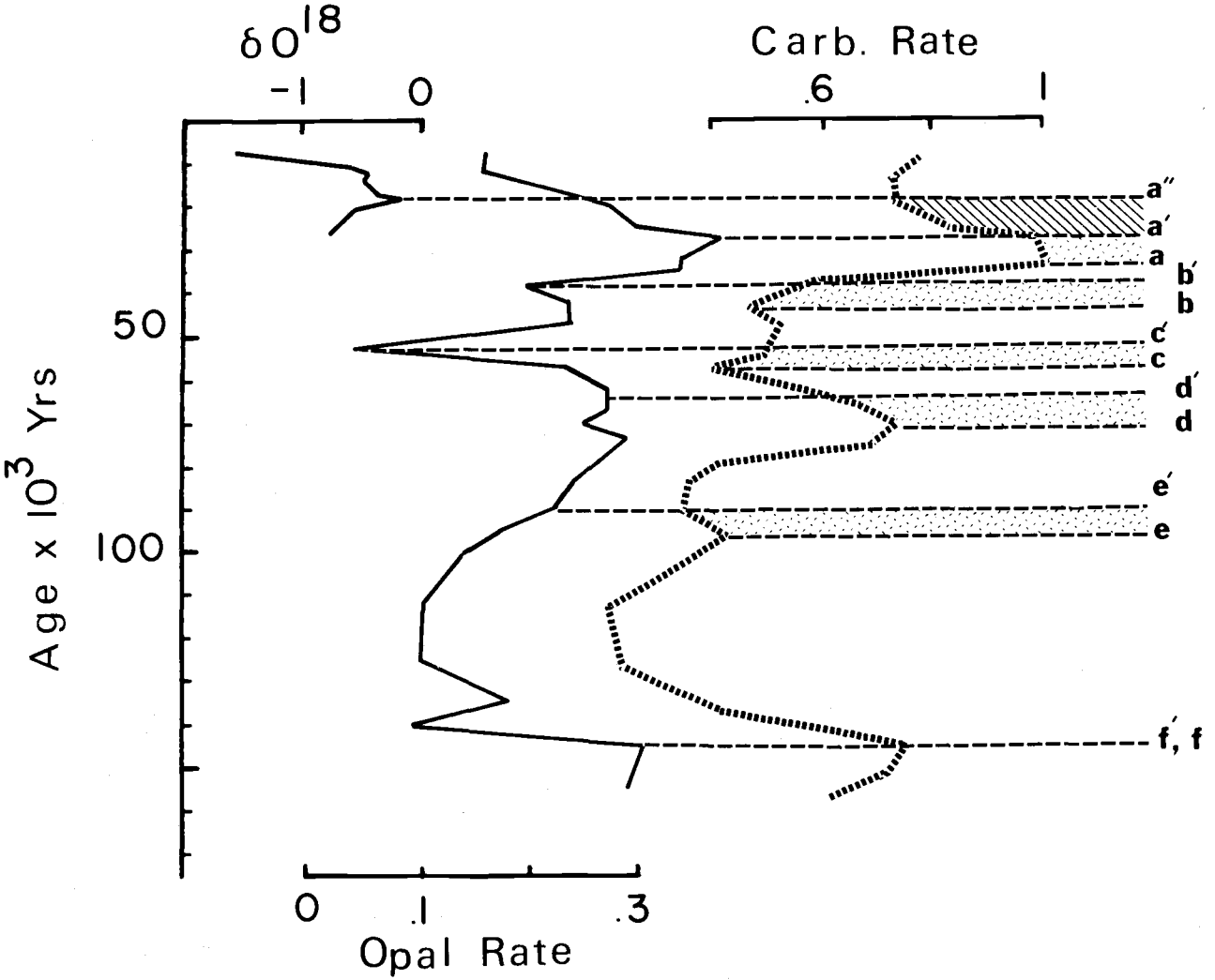

FIGURE 8 Lag time between carbonate and opal accumulation rates and oxygen isotope ratios of core Y69-106P.

circulation (opal rates) (Figure 8, a-f) is 2600 years.

In general, accumulation rates of calcium carbonate show very good correlation with oxygen isotope data, an indicator of global climatic change. Opal accumulation rates show good correlations with indicators of surface circulation, suggesting that biological productivity is the primary controlling factor of opal rates. The calcium carbonate accumulation rates, the opaline silica rates, and oxygen isotope data from core Y69-106P indicate that a sequence of events occurred during the transition from the last glacial to the present interglacial (Figure 8, a, a', a'') period. A change in the characteristics of the bottom water, (indicated by the calcium carbonate rates) precedes a change in surface circulation (indicated by the opal rates) and finally the continental glaciers began to recede (indicated by the oxygen isotopes). The time span of this sequence is 5600 years with about 2600 years elapsing between the bottom water and surface current changes and 3000 years between the change in surface currents and the recession of the continental glaciers. Because of the relatively wide spacing in time of individual samples (about 4000 years) these must be taken as upper-limit estimates.

Spectral Analysis of Y69-106P and V28-238 Climatic Records

Of major interest in the study and prediction of climatic

change through time is whether observed fluctuations are random or have periodic characteristics, and if periodicities do occur in climatic change whether they can be related to known periodic phenomenon. Climatic fluctuations have been measured on scales ranging from a year to hundreds of thousands of years. Major climatic cycles (glacial and interglacial stages) have been attributed to periodic changes in the orbital parameters of the earth relative to the sun (Milankovitch, 1938). Shorter-term climatic changes measured in centuries such as the "little" ice age of the fifteenth and sixteenth centuries have been attributed to changes in solar activity (Bray, 1968). According to Suess (1970) the variations in solar activity during the last 7,000 years is also periodic. Because the sun is the ultimate source of energy for the earth's oceans and atmosphere the periodic characteristics of solar activity and the earth's orbit should then be evident in climatic records.

Spectral analysis has proved to be very useful in examining the periodic character of paleoclimatic data: analysis of fluctuations in the carbon-14 content of the atmosphere, a measure of solar activity, points to the existence of 100, 400, and 2400 year periodicities (Suess, 1970). Analysis of data from an ice core from the Greenland ice sheet (Dansgaard et al., 1971) indicate a 380 year period, and studies of fluctuation in the extent of mountain glaciers point to a 2400 year period (Denton, 1972). Spectral

analysis of data obtained from deep-sea sediment cores has confirmed the existence of periodicities of a 400 and 2600 years previously observed in carbon-14 and mountain glacier data (Pisias et al., 1973), and has shown the presence of earth orbital parameter periodicities, 24,000 and 100,000 years, in a paleotemperature curve determined from a sediment core (Imbrie and Kipp, 1973).

To be amenable to the statistical technique of spectral analysis a time series must be a random variable or non-deterministic function of time. One characteristic of such a time series is that its future values cannot be precisely predicted. If the values of the time series at a given point can be described by a random variable and its associated probability distribution, the time series is said to be a stochastic process; the process is stationary if the statistical distribution of the random variable does not change with time. The paleoclimatic records are assumed to represent a stationary process, that is, the mechanisms controlling climatic fluctuations have remained uniform during the observed record.

Spectral analyses of the oxygen isotope curve of core V28-238 and the sedimentation rate curves of Y69-106P were carried out to test for periodicities in depositional events. The analyses were performed using the procedures described by Jenkins and Watts (1968). These procedures consist of first subtracting the mean of

the data set and then removing any linear trend to elminate non-stationarity due to changes in the mean with time. The autocorrelation function of the resulting time series is then calculated. The autocorrelation function is a function of "lags" which are integers greater than or equal to zero. At lag zero the function is equal to one (the correlation of the data set with itself), at lag 2 the function is equal to the correlation value between each sample point and its neighbor, and for lag k the function is the correlation value between each data point and the data point k time intervals away. If the data set is "noise" (the value of each data point is completely independent of any other), the autocorrelation function will be equal to one at lag zero and zero at all other lags. Fourier transformation of the autocorrelation function gives the estimated sample spectrum for the data set. The fourier transform describes the distribution of the variance of the data as a function of frequency. The fourier transform of the autocorrelation function is smoothed by a weighted moving average (data window) and confidence intervals for the spectral estimates are determined as a function of the length of the original data set, the number of lags of the autocorrelation function used to calculate the fourier transform, and the particular data window used. The longer the data set and the fewer lags of the autocorrelation function used (the narrower the window) the smaller the confidence interval.

The most convenient presentation of the results of spectral

analysis is a plot of the logarithm of the spectrum as a function of frequency, which is usually expressed as cycles per sample interval. If the original data is "noise", the spectrum is a constant function of frequency. Data sets with periodic characteristics have a spectrum with isolated highs or peaks centered around the frequency corresponding to the dominant period. The "significance" of a spectral peak is determined by using a window closing technique (Jenkins and Watts, 1968). With a large window, the spectrum is highly smoothed and confidence intervals relatively small. As the window is closed the spectrum becomes less smoothed and the confidence interval increases in magnitude. Spectral peaks which stay above the confidence interval and remain centered about the same frequencies while the window is closed are considered to represent significant periodicities in the data set.

The numerical techniques used to analyze a time series require that data be sampled at equal time intervals. In the case of a sediment core, this requires that the age of the sediment as a function of depth be known, a basic goal of the sedimentation rate model developed for Y69-106P. In general, cores are sampled at constant depth intervals and only later is a time scale attached to these samples. If the sedimentation rate varies with time, as it

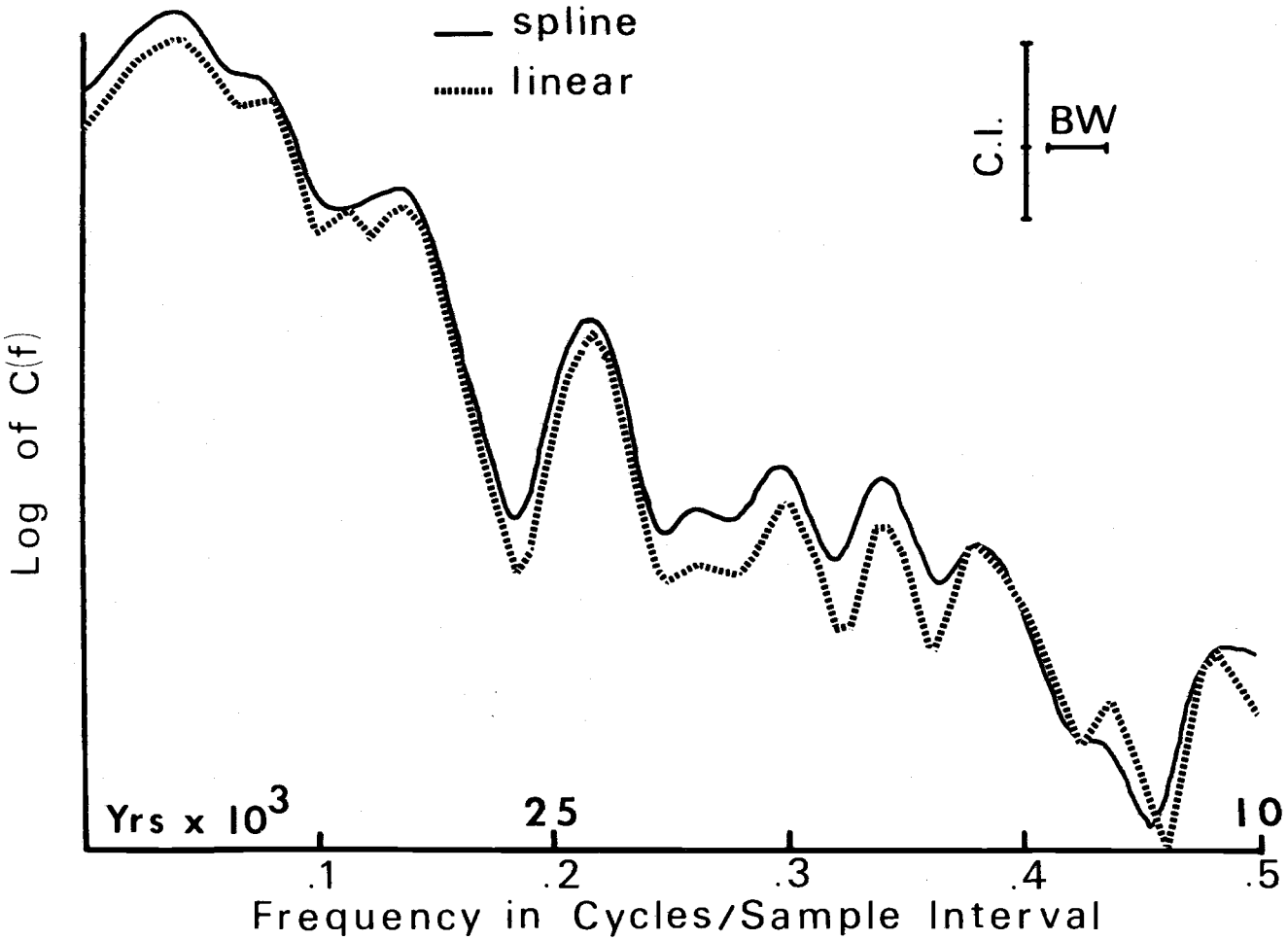

FIGURE 9 Spectra of V28-238 oxygen isotope data interpolated by spline and linear interpolation. C.I. 80% confidence interval, BW bandwidth, C(f) spectral estimate at frequency f. Note significant peak at 23,000 year period.

does in the cores studied here, then samples at constant depth intervals do not represent constant time intervals. If the time scale is reliable, either the core must be resampled, or, more realistically, interpolated data values must be generated at constant time intervals. Interpolation of points must not interfere with the spectrum of a data set by suppressing particular periods or by superimposing a period in the spectrum of the data. Two interpolation procedures were applied to the oxygen isotope data for V28-238 to check for interference by interpolation. The first procedure, a linear interpolation, is performed by drawing lines between successive data points and determining a value for any point from these lines. The second interpolation procedure makes use of a spline fit. The spline fit is a calculation of a third order polynomial between four successive points with the restriction that at each point the first and second derivative be mathematically continuous. A value of a point between any two data point is calculated using the polynomial determined by this procedure.

The oxygen isotope from core V28-238 was interpolated to a 5000 year sample interval by both interpolation techniques. The spectra obtained from the two interpolations are essentially the same (Figure 9) and both have a "significant" peak corresponding to a period of 23,000 years.

The calcium carbonate accumulation curve of core Y69-106P

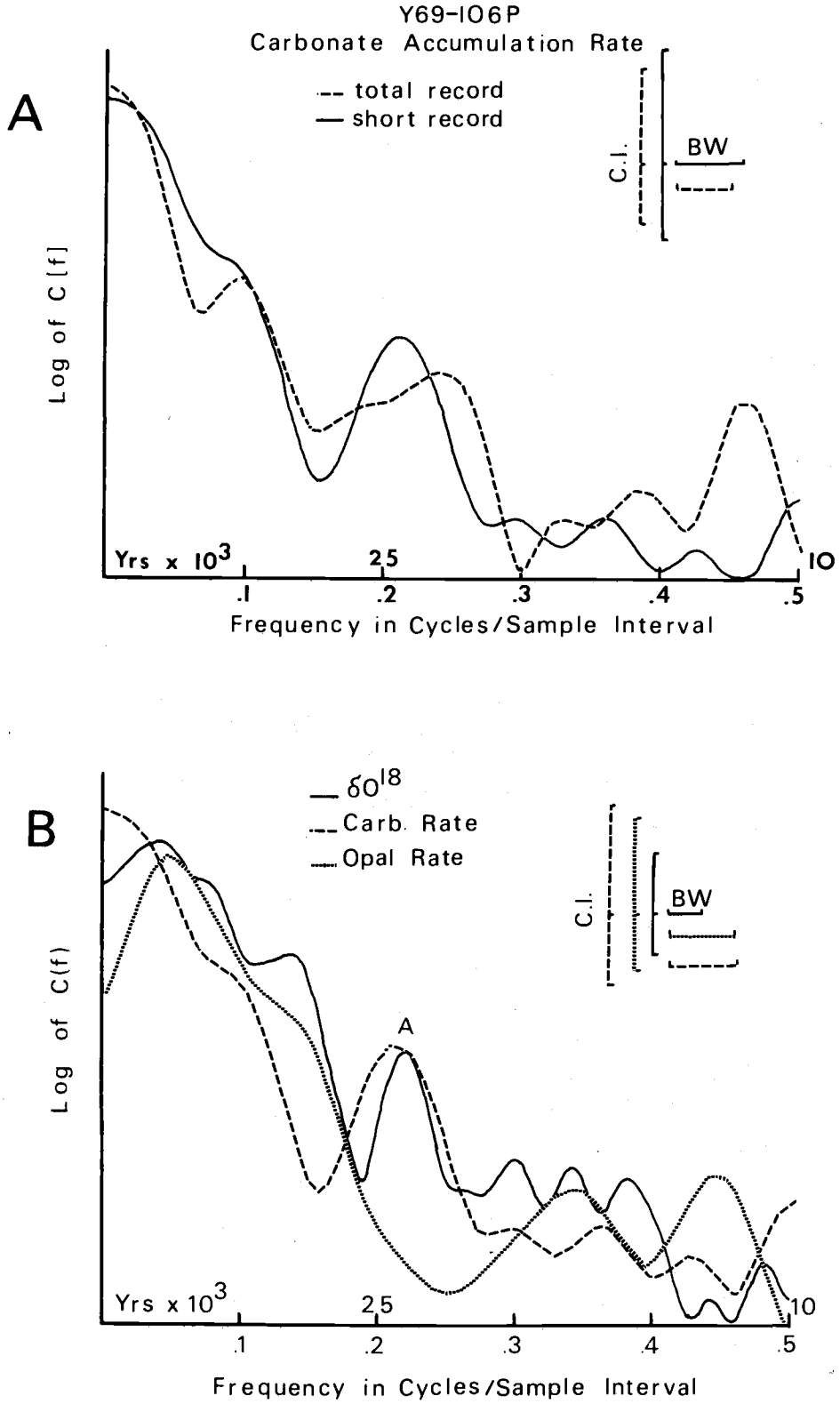

FIGURE 10 A. Spectral estimates for carbonate accumulation rates from Y69-106P for entire and shortened record.
B. Spectral estimates of shortened opal and carbonate accumulation rates from Y69-106P and oxygen isotope of V28-238. Annotation as in Figure 9.

was interpolated to a 5000 year sample interval using a polynomial spline fit. The lower part of the sedimentation rate curves of this core represent different conditions of sedimentation than the younger section, and thus represent a non-stationarity in the series. The spectra of the entire record of calcium carbonate accumulation and of the record representing the time from the present to 350,000 e. y. are different (Figure 10A). The spectrum of the shortened record of calcium carbonate has a peak at the frequency corresponding to a 23,000 year period, the same peak found in the V28-238 oxygen isotope data (Figure 10B).

In Figure 11 the spectra of calcium carbonate accumulation rate and concentration versus model age, and concentration versus age estimated by linear interpolation between dated samples, are compared. The spectra of concentrations are very similar for the two time scales, with the spectra based on the model ages shifted slightly towards lower frequencies. Neither of these spectra show the 23,000 year period observed in the calcium carbonate accumulation rate spectra. Thus, for this core, fluctuations in the calcium carbonate accumulation rate are a better guide to the climatic control of the oceanic carbonate system than are fluctuations in calcium carbonate concentration through time.

The spectral estimates of a shortened opal accumulation record (0 to 350,000 e. y.) does not indicate the presence of an

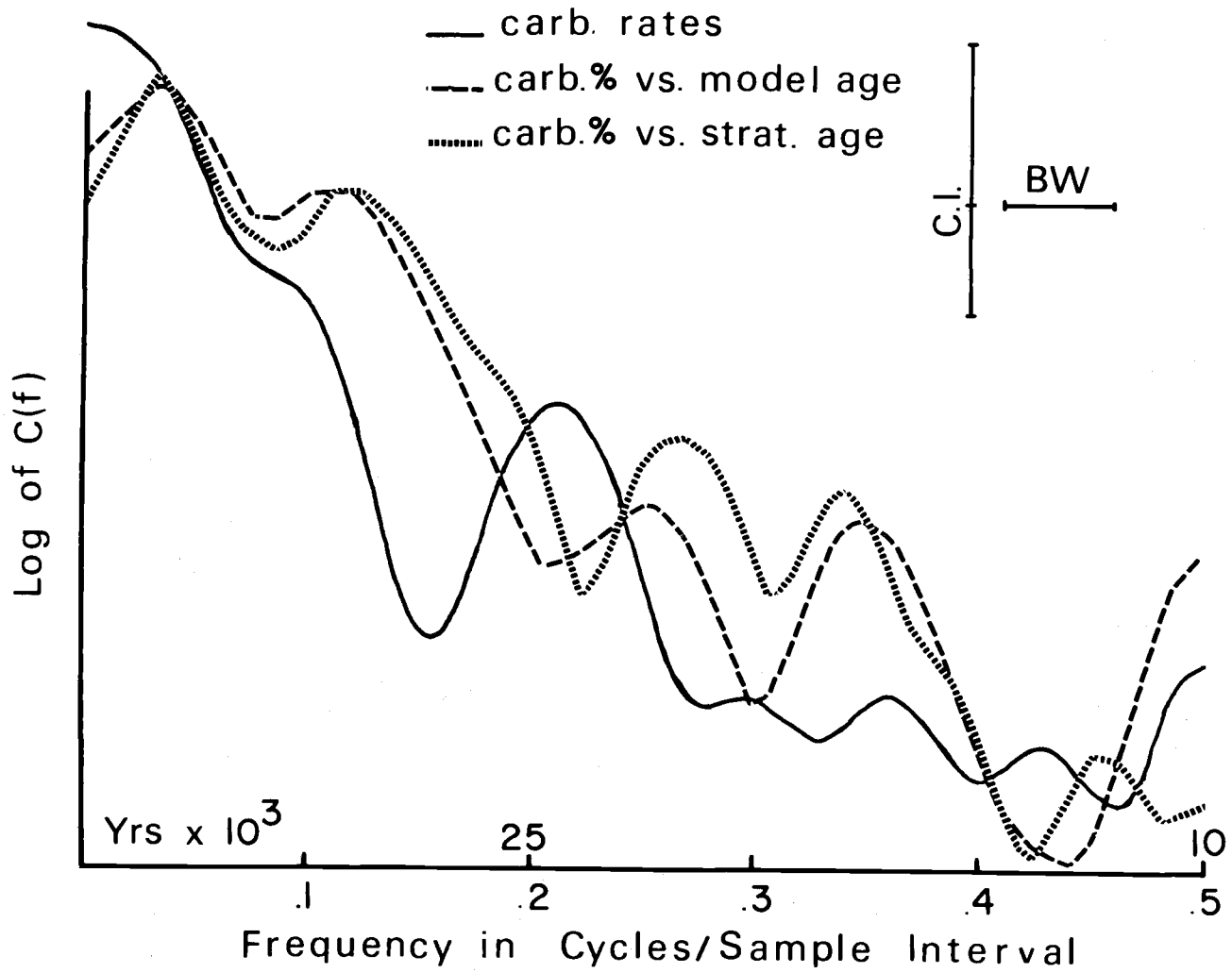

FIGURE 11 Spectral estimates of carbonate accumulation rate, carbonate concentration versus model age, and carbonate concentration versus stratigraphic age. Annotation as in Figure 9.

important periodicity at 23,000 years (Figure 10B). The opal spectrum does have an isolated low frequency maximum centered at around 100,000 years, however. The other spectra in Figure 10B also have a large amount of variance explained by very low frequencies, but the spectra of calcium carbonate accumulation rates and oxygen isotope data lack well defined maxima corresponding to specific frequencies of importance.

Spectral analysis has identified the importance of two periodicities of 23,000 and 100,000 years, in climatically influenced sedimentary properties. These periodicities correspond to two of the three periodic fluctuations of the earth's orbital parameters about the sun: changes in the eccentricity of the orbit (98,000 year period), tilt of the rotational axis relative to the orbital plane (44,000 year period), and precession of the equinoxes (22,000 year period) (Imbrie and Kipp, 1973). Precession of the equinoxes varies the distance from the earth to the sun during particular seasons. Winters will be colder when they occur at aphelion (furthest from the sun), than when they occur at perihelion. When winter occurs at aphelion, the following summer occurs at perihelion and the seasonal contrast is a maximum. The opposite conditions occur if winter coincides with perihelion. The effects of precession of the equinoxes are out of phase in the northern and southern hemispheres. When one hemisphere has maximal seasonal contrast, the other has

minimal contrast.

Variations in the eccentricity of the earth's orbit, which have an average period of 98,000 years, modulate the effect of precession of the equinoxes. The closer the orbit is to a circle the less precession affects seasonal contrast, and the more elliptical the orbit the more important precession becomes.

Therefore, the fluctuations of oxygen isotope ratios and calcium carbonate accumulation rates, both controlled by the high latitude processes of ice cap size and bottom water circulation respectively, are related to the precession of the equinoxes. Changes in the opal accumulation rate are controlled by changes in low latitude surface circulation that appear to be related to the eccentricity of the earth's orbit and may be related to changes in the distribution of incoming radiation throughout the year.

CONCLUSIONS

1) The assumption of a constant rate of quartz accumulation during the past 350,000 years in the Panama Basin allows detailed profiles of calcium carbonate and opal accumulation rates to be calculated. The validity of such a model is confirmed by the uniform rates of accumulation of quartz during three independently dated intervals in core Y69-106P.

2) Fluctuations in calcium carbonate accumulation rates from core Y69-106P show a very close correlation with climatic indicators. Correlation with oxygen isotope curves from other deep-sea cores indicate that during glacial times calcium carbonate accumulation rates were higher than during interglacial periods. Fluctuations in opaline silica rates parallel faunal changes that are related to local surface circulation. During periods of increased upwelling associated with the equatorial undercurrent, opal accumulation rates are high. Correlations between radiolarian assemblages and the accumulation of opaline silica suggest that changes in the rate of opal supply from surface waters is the primary factor controlling opal accumulation rates.

3) The oxygen isotope, calcium carbonate rate, and opaline silica rate curves are strikingly similar. However, slight offsets between the curves suggest a time transgression of climatically

controlled events at the end of the last glacial period. The last maximum of the carbonate accumulation rate curve occurred about 24,000 years ago. This maximum slightly preceded the last opal maximum (during the last 150,000 years changes in carbonate accumulations rates have preceded changes in opal accumulation rates by an average of 2,600 years). 5,600 years after the decrease in the carbonate accumulation rate, the glaciers began to recede (about 17,900 years ago). This sequence of events suggests that the following order of changes occurs at the end of a glacial period: 1) bottom water in the Pacific becomes more corrosive to calcium carbonate, 2) the intensity of local surface circulation and upwelling in the eastern equatorial Pacific decreases and 3) continental ice caps recede.

4) Periodicities found in the fluctuations of the earth's orbital parameters are found in climatic records from core Y69-106P and V28-238. Spectral analysis indicates the presence of a 23,000 year period in oxygen isotope data from core V28-238 and in the carbonate accumulation rates of Y69-106P; opal accumulation rates from Y69-106P suggest the presence of a 100,000 year period. The 23,000 year period is equal to the periodicity found in the precession of the equinoxes and 100,000 years is the period of fluctuations in the eccentricity of the earth's orbit.

BIBLIOGRAPHY

Altschuler, Z.S., R.S. Clarke, Jr., and E.J. Young. 1958. Geochemistry of uranium in opalite and phosphates. U.S. Geol. Survey Prof. Paper 314-D:45-87.

Arrhenius, G. 1952. Sediment cores from the East Pacific: Swedish Deep-Sea Expedition Reports (1947-1948). 5:1-89.

Berger, W.H. 1970. Biogenous deep-sea sediments: fractionation by deep-sea circulation. Geol. Soc. Am. Bull. 81(5):1385-1402.

Berger, W.H. and G.R. Heath. 1968. Vertical mixing in pelagic sediments. J. Mar. Res. 26(2):134-142.

Bray, J.R. 1968. Glacial and solar activity since the fifth century BC and solar activity. Nature 220:672-674.

Brereton, N.R. 1970. Correction for interfering isotopes in the $^{40}Ar/^{39}Ar$ dating method. Earth Planet. Sci. Let. 8:427-433.

Broecker, W.S. 1971. Calcite accumulation rates and glacial to interglacial changes in oceanic mixing. In: The Late Cenozoic Glacial Ages, K. Turekian, ed. Yale University Press.

Broecker, W.S., K.K. Turekian, and B.C. Heezen. 1958. The relation of deep-sea sedimentation rates to variations in climate. Am. J. Sci. 256:503-517.

Broecker, W.S. and J. van Donk. 1970. Insolation changes, ice volumes, and O^{18} record in deep-sea cores. Review of Geophys. and Space Phy. 8(1):169-198.

Calvert, S.E. 1966. Accumulation of diatomaceous silica in the sediments of the Gulf of California. Geol. Soc. Am. Bull. 77:589-596.

Dansgaard, W.S., S.J. Johnsen, H.B. Clausen, and C.C. Langway. 1971. Climatic record revealed by the Camp Century ice core. In: The Late Cenozoic Glacial Ages, K. Turekian, ed. Yale University Press.

Denton, G. H. 1972. Holocene glacier fluctuations and their possible cause. Geol. Soc. Am. Abstracts 4(7):487.

Dinkelman, M. G. 1974. Late Quaternary radiolarian paleo-oceanography of the Panama Basin, eastern equatorial Pacific. Ph. D. Thesis, Oregon State University, Corvallis. 123 numb. leaves.

Ellis, D. B. 1972. Holocene sediment of the South Atlantic ocean: the calcite compensation depth and concentration of calcite, opal, and quartz. Master's Thesis. Oregon State University, Corvallis. 77 numb. leaves.

Emiliani, C. 1955. Pleistocene temperatures. J. Geol. 63(6):539-578.

Ericson, D. B., M. Ewing, G. Wollin, and B. C. Heezen. 1961. Atlantic deep-sea sediment cores. Geol. Soc. Am. Bull. 72(2):193-286.

Fritts, H. C., T. J. Blasing, B. P. Hayden, and J. E. Kutzbach. 1971. Multivariate techniques for specifying tree-growth and climate relationships for reconstructing anomalies in paleo-climate. J. Applied Meteor. 10(5):845-864.

Goldberg, E. D. 1958. Determination of opal in marine sediments. J. Mar. Res. 17:178-192.

Goldberg, E. D. 1963. Geochronology with lead-210. In: Radioactive Dating, International Atomic Energy Agency, Vienna. p. 121-131.

Hays, J. D. 1970. Stratigraphy and evolutionary trends of radiolaria in North Pacific deep-sea sediments. Geol. Soc. Am. Mem. 126:185-218.

Hays, J. D. and D. Ninkovitch. 1970. North Pacific deep-sea ash chronology and age of the present Aleutian underthrusting. Geol. Soc. Am. Mem. 126:263-290.

Hays, J. D., T. Saito, N. D. Opdyke, and L. H. Burckle. 1969. Pliocene-Pleistocene sediments of the equatorial Pacific: their paleomagnetic, biostratigraphic, and climatic record. Geol. Soc. Am. Bull. 80(8):1481-1514.

Heath, G.R. 1974. Dissolved silica and deep-sea sediments. In: Studies in paleo-oceanography, W.H. Hay, ed. SEPM Special Publ. In press.

Heath, G.R., T.C. Moore, Jr. and G.L. Roberts. 1974. Mineralogy of surface sediments from the Panama Basin, eastern equatorial Pacific. J. Geol. 81. In press.

Imbrie, J. and N.G. Kipp. 1971. A new micropaleontological method for quantitative paleoclimatology: application to a late Pleistocene Caribbean core. In: The Late Cenozoic Glacial Ages, K. Turekian, ed. Yale University Press.

Imbrie, J., J. Van Donk and N. Kipp. 1973. Paleoclimatic investigation of Late Pleistocene Caribbean deep-sea core: comparison of isotopic and faunal methods. Quaternary Res. 3(1):10-38.

Jenkins, G.M. and D.G. Watts. 1968. Spectral Analysis and its Application. Holden-Day, 525 pp.

Klovan, J.E. and J. Imbrie. 1971. An algorithm and FORTRAN-IV program for large-scale Q-mode factor analysis and calculation of factor scores. Mathematical Geol. 3(1):61-77.

Kowsmann, R.O. 1973. Panama Basin surface sediments: coarse components. Master's Thesis. Oregon State University, Corvallis. 73 numb. leaves.

Ku, T.L. 1966. Uranium disequilibrium in deep-sea sediments. Ph. D. Thesis. Columbia University, New York. 157 numb. leaves.

Ku, T.L., W.S. Broecker, and N. Opdyke. 1968. Comparison of sedimentation rates measured by paleomagnetic and the ionium methods of age determination. Earth and Planetary Sci. Let. 4:1-66.

Laird, N.P. 1971. Panama Basin deep water properties and circulation. J. Mar. Res. 29:226-234.

Luz, B. 1973. Stratigraphic and paleoclimate analysis of late Pleistocene tropical southeast Pacific cores. Quaternary Res. 3(1):56-72.

McIntyre, A., W. F. Ruddiman, and R. Jantzen. 1972. Southward penetration of the North Atlantic polar front: faunal and floral evidence of large-scale surface water mass movements over the last 225,000 years. Deep-Sea Res. 19:61-77.

Milankovitch, M. 1938. Die chronologie des Pleistocene. Bull. Acad. Sc. Math. Nat., Belgrad, 4:49.

Moore, T. C., Jr. 1973. Method of randomly distributing grains for microscopic examination. J. Sedimentary Petrology. 43(3):904-906.

Moore, T. C., Jr., G. R. Heath, and R. O. Kowsmann. 1973. Biogenic sediments of the Panama Basin. J. Geol. 81(4):458-494.

Phipps, J. B. 1974. Sediments and tectonics of the Gorda-Juan de Fuca Plate. Ph. D. Thesis. Oregon State University, Corvallis. 118 numb. leaves.

Pisias, N. G., J. P. Dauphin, and C. S. Sancetta. 1973. Spectral analysis of late Pleistocene-Holocene sediments. Quaternary Res. 3(1):3-9.

Plank, W. S., J. V. Zaneveld, and H. Pak. 1973. Distribution of suspended matter in the Panama Basin. J. Geophy. Res. 78(30):7113-7121.

Prospero, J. M. and E. Bonatti. 1969. Continental dust in the atmosphere of the eastern equatorial Pacific. J. Geophy. Res. 74:3362-3371.

Shackleton, N. J. and N. D. Opdyke. 1973. Oxygen isotope and paleomagnetic stratigraphy of equatorial Pacific core V28-238: oxygen isotope temperatures and ice volumes on 10^5 year scale. Quaternary Res. 3(1):39-55.

Suess, H. E. 1970. The three causes of secular C^{14} fluctuations, their amplitudes and time constants. Radiocarbon variations and absolute chronology, Nobel Symposium 12, I. U. Olsson, ed., Uppsala, 1969, Almquist and Wiksell, Stockholm, and Wiley, New York.

Thurber, D. L. 1963. Natural variations in the ratio of U^{234} to U^{238}. In: Radioactive Dating, International Atomic Energy

Agency, Vienna. p. 113-120.

van Andel, Tj. H. 1973. Texture and dispersal of sediments in the Panama Basin. J. Geol. 81(4):434-457.

van Andel, Tj. H., G.R. Heath, B.T. Malfait, D.F. Heinrichs, and J.I. Ewing. 1971. Tectonics of the Panama Basin, eastern equatorial Pacific. Geol. Soc. Am. Bull. 82(6):1489-1580.

Veeh, H.H. 1967. Deposition of uranium from the ocean. Earth and Planetary Sci. Let. 3(2):145-150.

Wiseman, J.D.H. 1956. The rates of accumulation of nitrogen and calcium carbonate on the equatorial Atlantic floor. Advan. Sci. (London). 12:579.

APPENDICES

APPENDIX I - Sediment Composition Data

Sediment Composition Data - Y69-106P

Depth (cm)	Carbonate	Opal	Opal (c. f.)	Quartz	Quartz (c. f.)	Detritus	Density (gm/cm^3)	
0	64.2953	20.6400	7.3695	2.4100	.8605	27.4748		
10.0000	69.6706	46.2400	14.0243	3.6300	1.1010	15.2041	.4648	*
21.0000	68.8372	46.5900	14.5187	6.1500	1.9165	14.7275	.4762	
30.0000	67.1704	56.9200	18.6866	4.2100	1.3821	12.7609	.4876	*
40.0000	63.8786	61.9000	22.3591	4.1600	1.5027	12.2596	.4990	
51.0000	64.7536	64.4000	22.6987	3.5900	1.2618	11.2859	.5387	*
61.0000	66.6287	74.3900	24.8249	3.6200	1.2080	7.3383	.5057	
71.0000	65.9620	64.0300	21.7945	2.9600	1.0075	11.2359	.4728	*
81.0000	67.0038	74.8300	24.6911	3.7900	1.2506	7.0546	.4793	
91.0000	52.5029	35.3800	16.8045	3.0900	1.4677	29.2250	.4857	*
101.0000	46.7943	44.1700	23.5010	3.5500	1.8886	27.8159	.5130	
111.0000	45.7942	37.4200	20.2838	2.7900	1.5123	32.4096	.5404	*
121.0000	52.9196	20.3100	9.5620	2.2900	1.0781	36.4402	.5148	
131.0000	30.3767	3.4100	2.3742	.9600	.6684	66.5808	.4893	*
141.0000	31.7934	28.5400	19.4662	2.7300	1.8620	46.8784	.4912	
151.0000	51.7112	51.8200	25.0233	2.8900	1.3955	21.8700	.4930	*
161.0000	58.4199	56.1500	23.3472	3.8100	1.5842	16.6487	.5190	
171.0000	58.6283	46.5700	19.2668	2.9400	1.2163	20.8886	.5450	*
181.0000	57.5449	55.1700	23.4225	3.2000	1.3586	17.6741	.4984	
191.0000	46.2943	52.5000	28.1955	3.5900	1.9280	23.5822	.4518	*
201.0000	46.4609	57.0200	30.5280	4.0900	2.1897	20.8214	.4693	
211.0000	43.6274	49.2200	27.7466	3.9600	2.2324	26.3937	.4868	*
221.0000	55.0031	47.9200	21.5625	4.0100	1.8044	21.6300	.5161	
231.0000	57.7949	51.4100	21.6976	6.1100	2.5787	17.9287	.5475	*
241.0000	52.7946	48.3000	22.8002	9.4100	4.4420	19.9632	.5401	
251.0000	56.0031	50.1900	22.0820	9.5900	4.2193	17.6956	.5327	*
261.0000	60.6284	67.2200	26.4656	5.8000	2.2836	10.6225	.5580	
271.0000	61.7951	22.3400	8.5350	3.6700	1.4021	28.2678	.5832	*
281.0000	64.6286	72.3400	25.5877	4.0500	1.4325	8.3512	.5640	
291.0000	65.0453	76.7300	26.8207	4.4100	1.5415	6.5925	.5449	*
301.0000	62.2535	77.0500	29.0837	4.2900	1.6193	7.0435	.5672	
311.0000	59.3367	79.3200	32.2541	4.7900	1.9478	6.4614	.5895	*
321.0000	60.2950	75.3600	29.9217	4.7800	1.8979	7.8854	.5360	
331.0000	57.6282	66.8400	28.3213	4.9400	2.0932	11.9573	.4824	*
341.0000	54.9614	64.0300	28.8382	4.9500	2.2294	13.9710	.5045	
351.0000	59.1283	67.0700	27.4126	6.6800	2.7302	10.7288	.5267	*
361.0000	63.2119	65.1300	23.9601	4.5200	1.6626	11.1652	.5403	
371.0000	64.0036	60.7400	21.8642	4.1600	1.4975	12.6347	.5539	*
381.0000	62.5035	56.1400	21.0505	4.5300	1.6986	14.7474	.5029	
391.0000	62.9619	62.9600	23.3192	4.3100	1.5963	12.1226	.4518	*
403.0000	46.7109	54.0200	28.7868	3.5800	1.9077	22.5946	.4564	
413.0000	43.2103	60.2300	34.2041	3.2600	1.8513	20.7337	.4749	*
421.0000	39.0439	52.8000	32.1848	3.1500	1.9201	26.8512	.4828	
431.0000	33.0852	63.4600	42.4641	3.9100	2.6164	21.8343	.4907	*
441.0000	56.6282	37.0500	16.0693	3.0500	1.3228	25.9797	.4840	
451.0000	49.2944	49.8000	25.2514	4.1000	2.0789	23.3753	.4773	*
461.0000	54.7947	49.1900	22.2365	4.2100	1.9031	21.0657	.4852	
471.0000	60.4617	29.2400	11.5610	3.6900	1.4590	26.5183	.4931	*
481.0000	55.7115	40.1900	17.7995	4.3000	1.9044	24.5845	.5666	
491.0000	52.8363	26.9800	12.7248	3.4300	1.6177	32.8212	.6402	*
501.0000	43.2941	8.9500	5.0752	1.9200	1.0888	50.5420	.6593	
511.0000	1.6668	1.3700	1.3472	.0700	.0688	96.9172	.6765	*
521.0000	33.7936	19.4000	12.8440	2.1000	1.3903	51.9720	.6400	
531.0000	61.3784	33.0600	12.7683	5.2100	2.0122	23.8411	.6035	*
541.0000	65.8370	60.0300	22.5578	5.3500	1.8277	9.7775	.6166	
551.0000	68.4205	67.1400	21.2025	4.7900	1.5127	8.8644	.6298	*
561.0000	72.4207	62.9800	17.3694	4.1800	1.1528	9.0570	.5605	
571.0000	69.5456	78.3500	23.8610	3.9600	1.2060	5.3874	.4912	*
581.0000	55.7931	31.8600	14.0971	4.7400	2.0973	28.0525	.5559	
591.0000	60.5451	65.8700	25.9389	4.4600	1.7597	11.7063	.6206	*

Depth (cm)	Carbonate	Opal	Opal (c. f.)	Quartz	Quartz (c. f.)	Detritus	Density (gm/cm^3)	
601.0000	60.8784	30.1800	11.8069	3.6500	1.4279	25.8868	.6228	
611.0000	75.7126	91.7600	22.2961	3.7700	.9156	1.0856	.6251	*
621.0000	72.4624	82.6700	22.7653	3.5900	.9886	3.7837	.5636	
631.0000	71.7540	78.2500	22.1025	2.9600	.8078	5.3357	.6099	*
641.0000	68.1283	82.3900	26.2587	3.1700	1.0103	4.6022	.5625	
651.0000	68.5038	81.5700	25.6915	3.0600	.9638	4.8410	.5151	*
661.0000	58.5866	56.0200	23.1998	3.4700	1.4370	16.7766	.5749	
671.0000	64.1703	29.3000	10.4981	1.2600	.4515	24.8801	.6348	*
681.0000	73.6708	20.4200	5.3764	2.7600	.7267	20.2261	.6617	
691.0000	70.3373	53.4800	15.8636	4.9800	1.4772	12.3219	.6887	*
701.0000	73.7958	61.3500	16.0763	5.6300	1.4753	8.6526	.6961	
713.0000	76.5876	74.1800	17.3673	4.7900	1.1215	4.9236	.7035	*
721.0000	76.3793	74.4200	17.5785	3.9100	.9236	5.1186	.6451	
731.0000	71.4623	82.2700	23.4780	3.9100	1.1158	3.9439	.5913	*
741.0000	68.5455	79.0200	24.8553	4.4000	1.3840	5.2152	.5782	
751.0000	69.0455	80.0900	24.7915	4.6900	1.4518	4.7113	.5651	*
761.0000	68.3372	78.6700	24.9091	3.7400	1.1842	5.5695	.5360	
771.0000	71.1707	55.7500	16.0723	2.4000	.6919	12.0651	.5070	*
781.0000	69.4206	75.8600	23.1975	3.4600	1.0580	6.3238	.4809	
791.0000	68.5872	5.4500	1.7120	.9500	.2984	29.4024	.5003	*
801.0000	58.2116	60.7400	25.3823	3.1400	1.3122	15.0940	.4863	
811.0000	64.5453	55.4500	19.6596	2.7500	.9750	14.8201	.4724	*
821.0000	68.7538	66.7600	20.8600	3.0300	.9468	9.4395	.6301	
831.0000	70.6706	64.2000	18.8295	4.3500	1.2758	9.2241	.7039	*
841.0000	72.7124	83.0400	22.6596	4.3400	1.1843	3.4437	.7364	
851.0000	70.9623	44.6100	12.9537	4.0400	1.1731	14.9109	.7690	*
861.0000	75.2125	38.7800	9.6126	4.6800	1.1601	14.0149	.7676	
871.0000	73.4624	72.1600	19.1495	4.7400	1.2579	6.1302	.7663	*
881.0000	76.7126	74.5100	17.3514	5.6500	1.3157	4.6202	.7692	
891.0000	79.2128	76.6600	15.9355	5.3200	1.1059	3.7459	.7721	*
901.0000	78.3377	59.6800	12.9281	4.3900	.9510	7.7833	.7363	
911.0000	73.6708	36.2700	9.5496	2.0800	.5476	16.2320	.7004	*
921.0000	74.4625	57.7600	14.7505	2.3100	.5899	10.1971	.6943	
931.0000	74.0041	44.6400	11.6046	3.2600	.8475	13.5439	.6882	*
946.0000	78.2961	79.5600	17.2676	4.1100	.8920	3.5442	.6395	
951.0000	71.7957	81.4500	22.9724	4.9500	1.3961	3.8358		
961.0000	55.2948	80.6000	36.0324	3.5700	1.5960	7.0768		
971.0000	51.9612	78.8800	37.8930	3.3800	1.6237	8.5221		
983.0000	66.7954	71.4100	23.7114	4.5200	1.5008	7.9923		
991.0000	64.5036	71.2800	25.3018	5.0900	1.8068	8.3878		

(c. f. - percentage of carbonate free sediment; * interpolated value)

Sediment Composition Data - Y69-73P

Depth (cm)	Carbonate	Opal	Opal (c. f.)	Quartz	Quartz (c. f.)	Detritus
10.0000	74.4000	13.8100	3.5354	1.4700	.3763	21.6883
20.0000	74.7000	35.4400	8.9663	1.9700	.4984	15.8353
30.0000	75.0000	33.5900	8.3975	1.4800	.3700	16.2325
40.0000	71.4000	36.8400	10.5362	1.2600	.3604	17.7034
50.0000	68.3000	31.7600	10.0679	1.3700	.4343	21.1978
60.0000	68.4000	35.0700	11.0821	1.4800	.4677	20.0502
70.0000	74.3000	20.5700	5.2865	1.8600	.4780	19.9355
80.0000	76.7000	34.2400	7.9779	3.6400	.8481	14.4740
90.0000	77.6000	23.5500	5.2752	3.3400	.7482	16.3766
100.0000	78.5000	33.7000	7.2455	2.7400	.5891	13.6654
110.0000	75.0000	36.1100	9.0275	2.1400	.5350	15.4375
120.0000	73.3000	38.3700	10.2448	2.2600	.6034	15.8518
130.0000	72.3000	33.3200	9.2296	1.9600	.5429	17.9274
140.0000	75.3000	13.4800	3.3296	.8100	.2001	21.1704
150.0000	72.5000	23.2200	6.3855	1.3900	.3823	20.7322
160.0000	73.5000	34.8500	9.2352	1.9500	.5168	16.7480
170.0000	69.3000	33.8900	10.4042	1.5300	.4697	19.8261
180.0000	74.3000	31.9600	8.2137	1.2800	.3290	17.1573
190.0000	70.3000	36.6400	10.8821	2.8000	.8316	17.9863
200.0000	71.2000	27.6700	7.9690	1.4300	.4118	20.4192

(c. f. - percentage in carbonate free sediment)

APPENDIX II

Thorium-230 Activity data from core Y69-106P

The results of the Th^{230} activity measurements in samples from core Y69-106P are given in Table II-1. The logarithm of the Th^{230} activities in calcium carbonate-free sediment are plotted versus depth in the core in Figure II-1. Calculation of Th^{230} activity on a carbonate-free basis improves the linearity of the logarithm of the Th^{230} activity versus depth plot and thus the Th^{230} activity in carbonate-free sediment is used in the following calculations.

An average sedimentation rate of a core can be estimated from the plot of the logarithm of Th^{230} activity versus depth by use of the equation:

$$\ln A_T = -\frac{\lambda}{S} T(x) + \ln A_o$$

where A_o is the Th^{230} activity in recent sediment, A_T the Th^{230} activity in the sediment at depth x, S is the average sedimentation rate to depth x, and λ_T is the decay constant of Th^{230}, 9.22×10^{-6} yr^{-1} (Ku et al., 1968). For uniform sedimentation rates the $\ln A_T$ versus depth curve is a straight line with slope $-\lambda_T/S$. The slope of the least square line through the data points in Figure II-1 ($R = -.96$) gives an average sedimentation rate for core Y69-106P of 6.6 cm/1000 yrs. ($\pm$ 1.0 cm/1000 years).

The average sedimentation rate obtained from the Th^{230}

TABLE II-1

Thorium-230 activity in core Y69-106P

Depth (cm)	Th^{230} (dpm/gm.) (total sediment)	Carbonate %	Th^{230} (dpm/gm.) (carbonate free)
43.	3.51	68.83	9.72
78.5	3.26	66.37	9.70
147.5	4.16	49.75	8.29
183.5	3.91	55.83	8.85
209.5	4.32	46.02	7.88
385.5	2.48	65.43	7.21
422.5	3.87	39.22	7.70
478.5	2.15	58.33	5.18
583.5	2.11	55.93	4.79
658.5	1.61	61.29	4.16
758.5	1.20	69.08	3.88
783.5	0.91	68.33	2.87

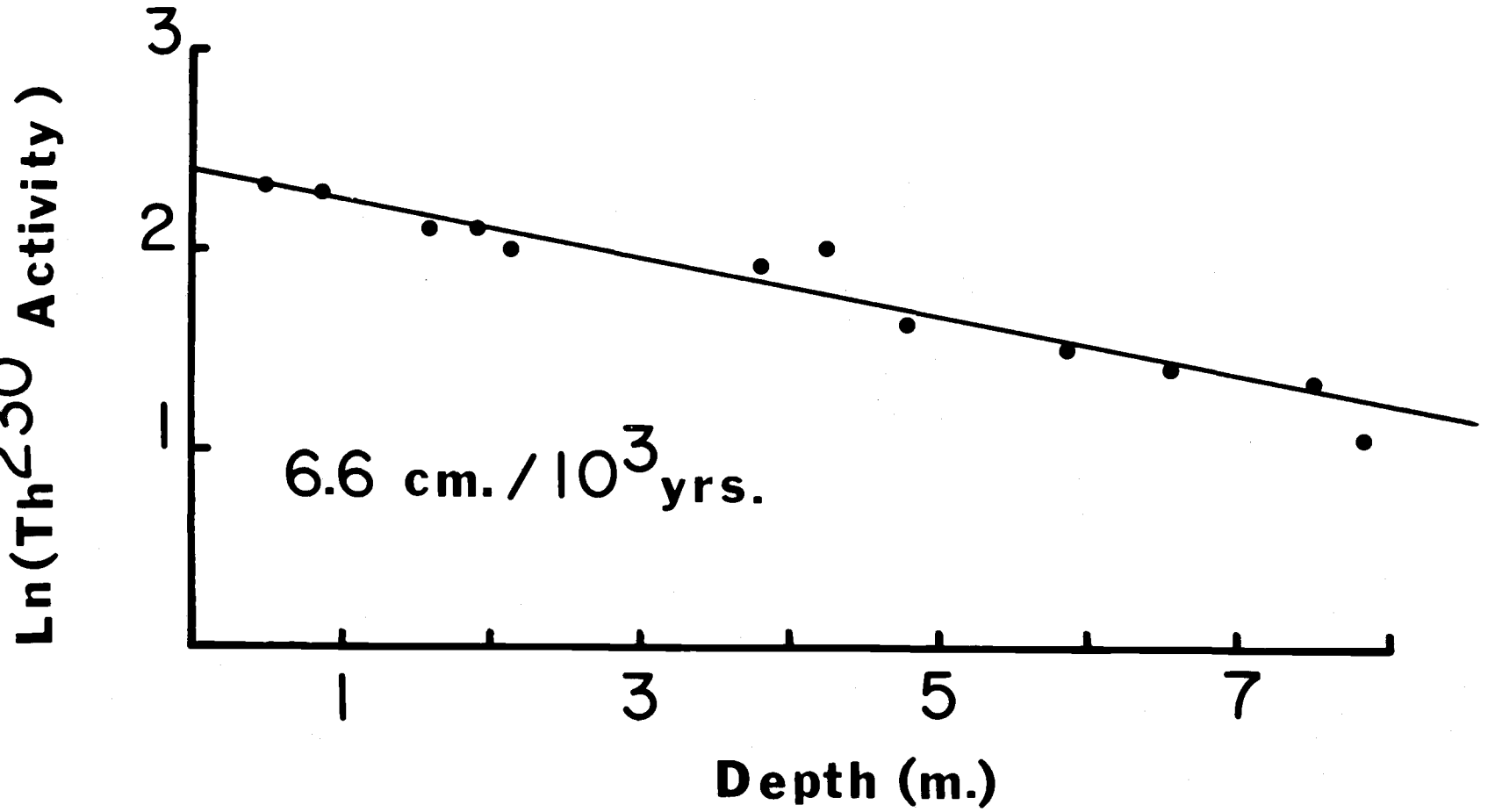

FIGURE II-1 Logarithm of Th^{230} activity versus depth in core Y69-106P.

analyses in core Y69-106P is three times larger than the rate determined by stratigraphic correlations, (twelve times greater than potassium argon dating of the volcanic ash at 506 cm depth in the core). The disagreement of the Th^{230} method with other techniques indicates that the initial assumptions of the method are not satisfied. These assumptions can be summarized as follows:

1) The amount of Th^{230} entering the surface sediment has remained constant over the time period of the core of interest.

2) The analyzed material does not contain detrital substances of continental or volcanic origin with significant amount of Th^{230}.

3) There is no migration of Th^{230} in the sediment.

4) Supported activity of uranium isotopes is assumed to be small or measurements are made to correct for Th^{230} activity due to uranium.

The measured Th^{230} activities in the samples from this core were not corrected for uranium-supported ionium. The sediment in Y69-106P is chemically reducing, a condition conducive to the precipitation of uranium (Veeh, 1967). Thus enrichment of uranium in this core may explain the high rate calculated from the Th^{230} data.

Th^{230} is the decay product of U^{234}, which in turn forms via series decay from U^{238}. Because of the much longer half life of U^{238} the two uranium isotopes should be in secular equilibrium, but since U^{234} is preferentially leached during weathering the activity

ratio of U^{234} to U^{238} in sea water is about 1.14 (Goldberg, 1963; Thurber, 1963). In freshly deposited sediment samples the total Th^{230} activity is equal to the sum of the activity due to direct precipitation of Th^{230} from sea water and the activity of Th^{230} supported by the decay of U^{234} (= 1.14 x U^{238} activity). With increasing age the uranium isotopes approach equilibrium and the activity due to Th^{230} originally precipitated from sea water becomes small, so that at ages greater than about 1,000,000 years the Th^{230} activity is equal to the activity of U^{238}.

Therefore if the uranium content of the sediment is not trivial some corrections for uranium-supported thorium activity must be made. To estimate whether uranium activity is a plausible cause for the high estimated sedimentation rates, the following assumptions have been made:

1) The Th^{230} activity measured in the oldest sample from the core is totally supported by U^{238}.

2) The concentration of U^{238} in the sediment (carbonate-free) is constant down the core. The sediments are uniformly reducing which should result in minimal migration of uranium (Altschuler et al., 1958).

3) The activity of U^{234} is initially equal to 1.14 times the U^{238} activity. From assumption 2) the initial U^{234} activity in the sediment is constant through time.

At any time the observed Th^{230} activity should be equal to the sum of the Th^{230} activity from the decay of the initial Th^{230} precipitated in the sediment, the Th^{230} activity due to the decay of U^{234} not in equilibrium with U^{238} and the Th^{230} supported by U^{238}.

In Figure II-2 the logarithm of the observed Th^{230} activity, A_{mt}, is plotted versus model ages in core Y69-106P. The regression line ($r = -.93$) describing these points gives an initial Th^{230} activity at time zero of 11.0 dpm/gm. Because of its long half life, U^{238} is taken to be a constant, 3.88 dpm/gm, down the core. The initial activity of U^{234} in a sample is 4.42 dpm/gm (1.14 x 3.88) and as shown in Figure II-2 decays with time to be in equilibrium with U^{238}. The initial activity of unsupported Th^{230} due to precipitation from sea water is 6.58 dpm/gm ($A_{tp} = 6.58 = 11.0 - 4.42$). The initial Th^{230} excess activity from sea water decays with time as follows:

$$A_{tt} = A_{tp} e^{\lambda_T T} \qquad (1)$$

where A_{tt} is the activity of Th^{230} at time T due to the decay of the precipitated Th^{230}; λ_T is the decay constant of Th^{230} (9.22×10^{-6}). The algebraic expression for the Th^{230} activity due to the decay of U^{234} not in equilibrium with U^{238} is:

$$A_{tu4} = \frac{14}{144} U_o^{234} (\lambda_U / (\lambda_T - \lambda_U))(e^{-\lambda_U T} - e^{-\lambda_T T}) \qquad (2)$$

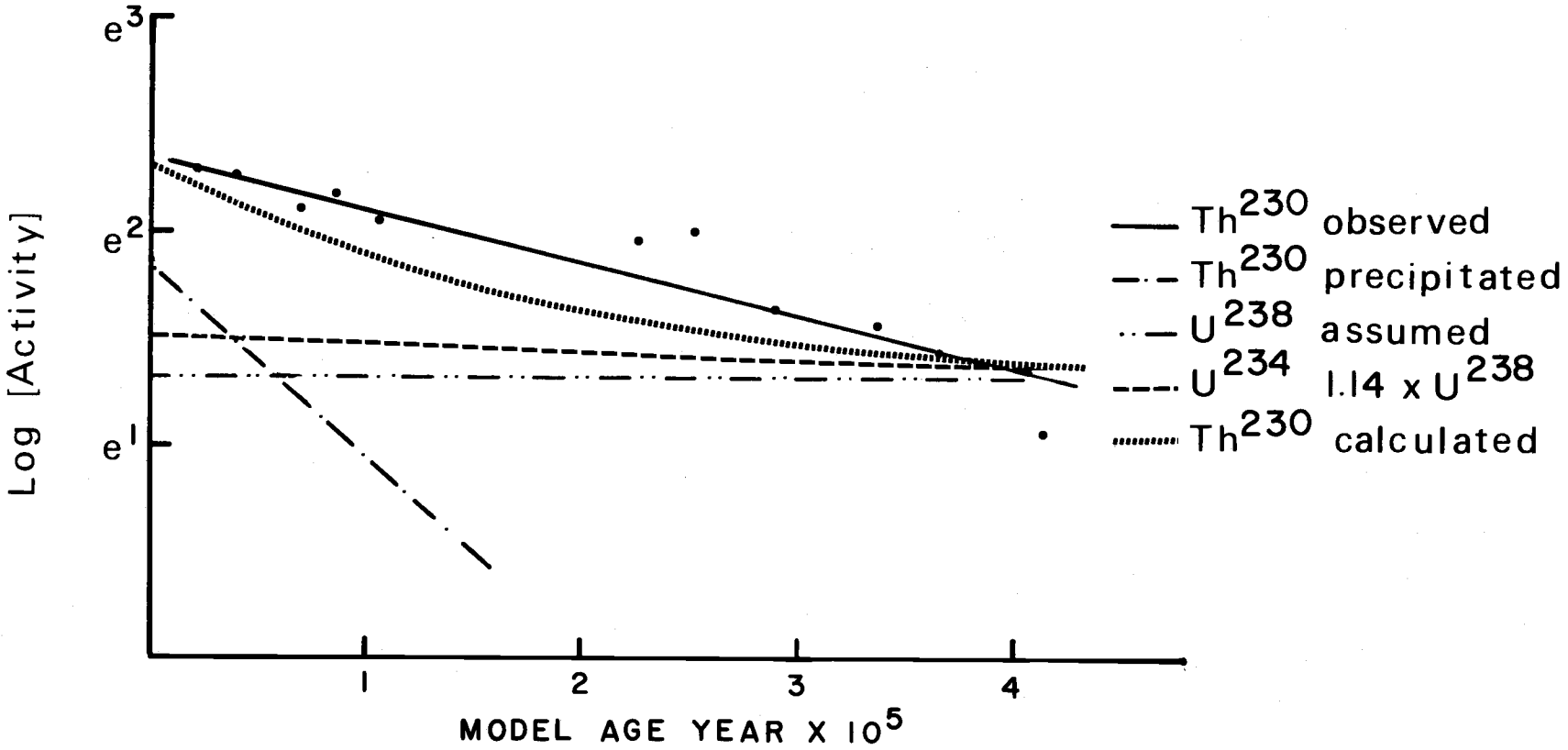

FIGURE II-2 Logarithm of Th^{230} activity versus sedimentation model age and calculated Th^{230} activity due to uranium supported Th^{230} activity.

where A_{tu4} is the supported Th^{230} activity due to U^{234} at time T, U_o^{234} is 4.42, and λ_U is the decay constant of U^{234} (2.77×10^{-6}). The sum of equations 1, 2 and the activity of U^{238} are plotted in Figure II-2. The disagreement between the calculated and observed data probably reflect non-uniform precipitation of uranium with time, or the presence of detrital substances with varying amount of Th^{230} activity. In the absence of uranium analysis this calculation suggests that supported Th^{230} is great enough in reduced sediments like those of Y69-106P to render raw Th^{230} activity data unsuitable for sedimentation rate determinations.

APPENDIX III

Extinction of the radiolarian Stylatractus universus

Sample slides were prepared by the random mounting procedure outlined by Moore (1973), and the total number of S. universus was counted in each sample slide. The total number of radiolarian tests on a slide was determined by counting the number of tests in a known area of the slide. At least 1000 tests were counted in this subsample. The results of the counts are given in Figure IV-1. S. universus was not found in samples from 800 - 829 cm depths in the core or in the upper three meters of the core (Dinkelman, written comm., 1973). Samples between 300 and 800 cm were not examined. From Figure IV-1 the extinction level was determined using the sediment mixing model described by Berger and Heath (1968). The extinction level is taken to be 841 cm depth in the core Y69-106P.

TABLE IV-1

S. universus in core Y69-106P

Depth in Core (cm)	S. universus/1000 radiolarian
800	0
829	0
836	0.4
842	1.2
863	2.8
869	2.0
874	3.2

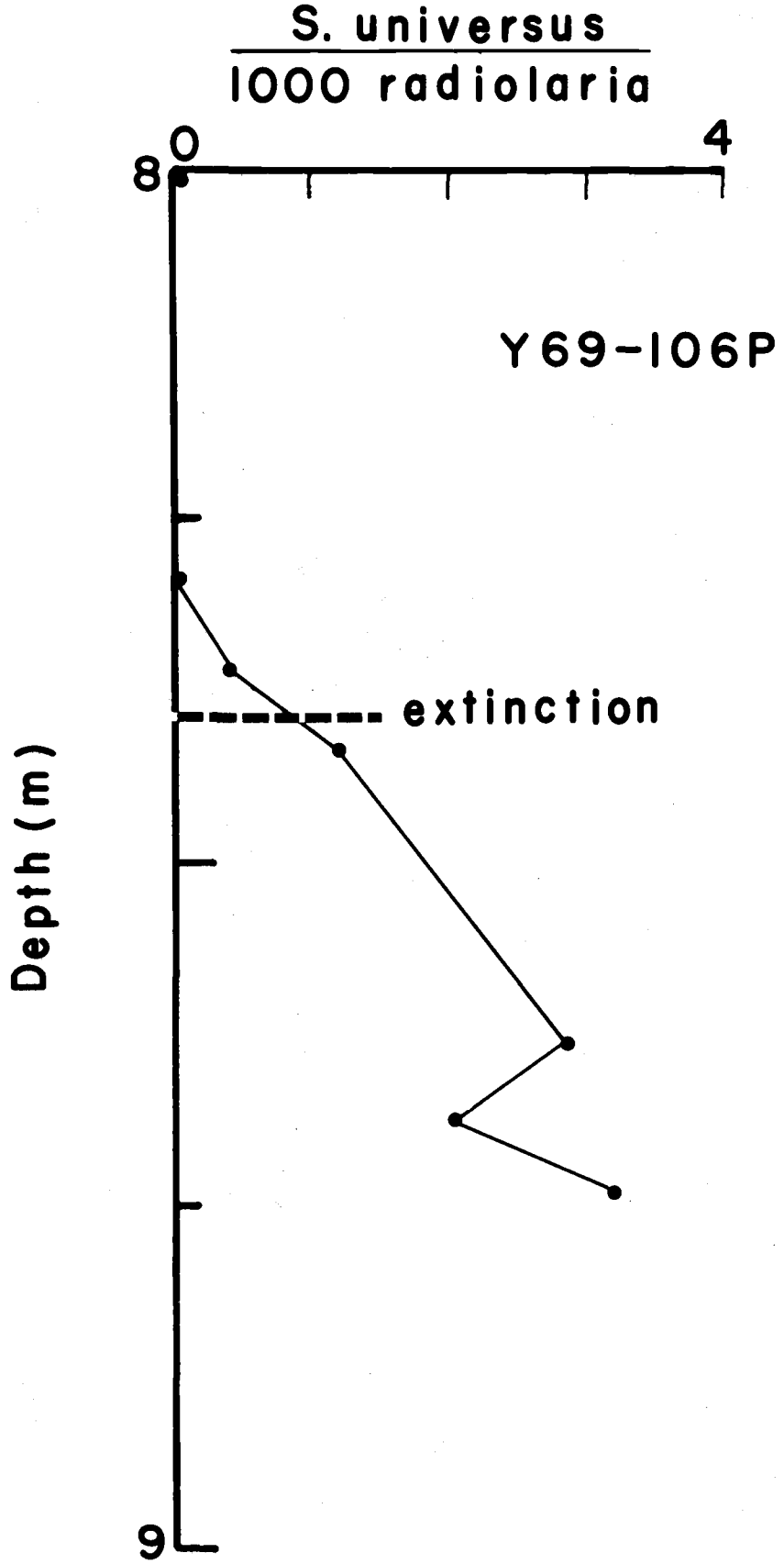

FIGURE III-1 Extinction of radiolarian S. universus in Y69-106P.

APPENDIX IV

Assumption of Constant Quartz Accumulation Applied to Y69-73P

As previously discussed, core Y69-73 was taken in the Panama Basin in the area of the Galapagos Rift Zone (Figure 1). This core has a sedimentation rate four times greater than that of Y69-106P. Bulk density values were not measured for this core so the mean value of the bulk densities from Y69-106P (.566 gm/cm^3) was combined with the quartz concentration data from Y69-73P to estimate the quartz mass versus depth curve and an age model using the assumption of constant quartz accumulation. A carbon-14 measurement at 50 cm depth (8,900 years) and the 17,900 year datum corresponding to the youngest oxygen isotope maximum at 130 cm depth (N. Shackleton, written comm., 1973) were used as calibration points. The surface age estimated by the model is 3605 e. y., within the error limits of the carbon-14 date for the 0 to 5 cm interval. The model ages have been used to calculate the sedimentation rates of calcium carbonate, opaline silica, and "detritus" in the core (Figure IV-1 and Appendix IV).

The rates of accumulation of calcium carbonate and "detritus" closely parallel each other (Figure 12). Peaks at 19,000 e. y. in the carbonate and "detritus" rates coincide with a low in the opal accumulation rate curve, suggesting that this interval is rich in

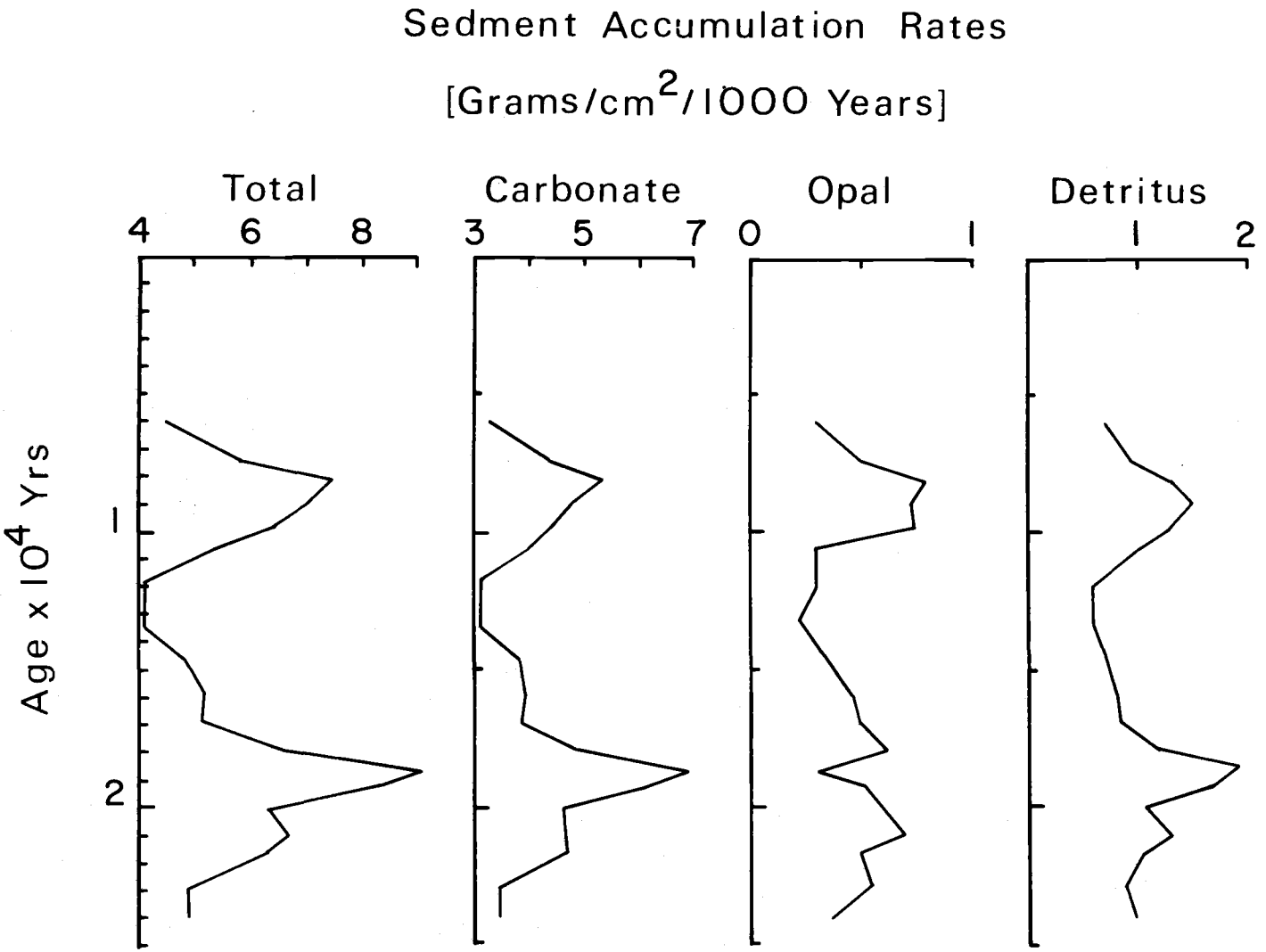

FIGURE IV-1 Model accumulation rates for Y69-73P.

reworked material. The interval of rapid carbonate and "detritus" accumulation at 9,000 e. y., with no associated opal accumulation low, may also reflect reworking. Differences in the oxygen isotopic composition of planktonic and benthic foraminifera from the same samples support the possibility of reworking at both of the highs in the "detritus" curve (N. Shackleton, written comm., 1973).

If much of the sediment in this core is reworked, the assumption of a constant rate of quartz accumulation is probably not valid at this location. However, the model does seem to reveal intervals of extensive reworking which are verified by the independent oxygen isotope data. It may be that the location of the core close to the quartz-poor Galapagos pedestal allows material derived from the pedestal to be distinguished from the more truly "pelagic" quartz.

APPENDIX V

Accumulation rates for Y69-106P

(grams/cm^2/1000 years)

Sample Depth (cm)	Age (yrs.)	cm/1000 yrs	Total Rate	Carbonate	Opal	"Detritus"
10	8036	2.4899	1.1695	.8148	.1640	.1778
21	12454	2.3765	1.1046	.7604	.1604	.1627
30	16431	2.3917	1.1389	.7650	.2128	.1453
40	20398	2.5468	1.2418	.7933	.2777	.1522
51	24673	2.6557	1.3252	.8581	.3008	.1496
61	28325	2.8798	1.5513	1.0336	.3851	.1138
71	31635	3.1030	1.5692	1.0351	.3420	.1763
81	34775	2.9460	1.3929	.9333	.3439	.0983
91	38468	2.4351	1.1671	.6128	.1961	.3411
101	43092	2.1166	1.0280	.4811	.2416	.2860
111	47922	2.3255	1.1930	.5463	.2420	.3866
121	51797	3.1618	1.7194	.9099	.1644	.6266
131	54441	3.2878	1.6926	.5141	.0402	1.1269
141	58021	2.4942	1.2204	.3880	.2376	.5721
151	62576	2.2930	1.1263	.5824	.2818	.2463
161	66759	2.4363	1.2011	.7017	.2804	.2000
171	70788	2.5189	1.3073	.7665	.2519	.2731
181	74701	2.3081	1.2579	.7239	.2946	.2223
191	78554	1.9290	.9614	.4451	.2711	.2267
201	85117	1.7602	.7953	.3695	.2428	.1656
211	90921	1.7743	.8309	.3625	.2305	.2193
221	96399	1.7075	.8278	.4553	.1785	.1791
231	102691	1.2605	.6505	.3760	.1412	.1166
241	113425	.8379	.4588	.2422	.1046	.0916
251	126863	.8735	.4718	.2642	.1042	.0835
261	136833	1.3783	.7342	.4451	.1943	.0780
271	142536	1.9603	1.0938	.6759	.0934	.3092
281	147150	2.1116	1.2315	.7959	.3151	.1028
291	152014	2.0287	1.1442	.7442	.3069	.0754
301	157011	1.8826	1.0258	.6386	.2983	.0723
311	162679	1.6703	.9474	.5622	.3056	.0612
321	169022	1.5705	.9258	.5582	.2770	.0730
331	175415	1.5798	.8468	.4880	.2398	.1013
341	181683	1.5122	.7295	.4009	.2104	.1019
351	188680	1.4925	.7530	.4452	.2064	.0808
361	195108	1.8182	.9576	.6053	.2295	.1069
371	199914	2.0419	1.1032	.7061	.2412	.1394
381	204906	2.0068	1.1116	.6948	.2340	.1639
391	209880	2.0581	1.0350	.6517	.2414	.1255
403	215579	2.0799	.9397	.4389	.2705	.2123
413	220448	2.0247	.9241	.3993	.3161	.1916
421	224457	1.8036	.8565	.3344	.2757	.2300
431	230661	1.7224	.8316	.2751	.3531	.1816
441	236116	1.9755	.9694	.5489	.1558	.2518
451	240838	1.9744	.9556	.4711	.2413	.2234
461	246300	2.0000	.9546	.5231	.2123	.2011
471	250910	2.1487	1.0425	.6303	.1205	.2765
481	255608	2.0088	.9905	.5518	.1763	.2435
491	260902	2.0308	1.1507	.6080	.1464	.3777
501	265505	3.4476	2.2072	.9556	.1120	1.1155
511	267622	4.1393	2.7249	.0454	.0367	2.6409
521	270434	2.5646	1.7350	.5863	.2228	.9017
531	276791	1.5197	.9726	.5970	.1242	.2319
541	283611	1.5942	.9621	.6334	.2170	.0941
551	289416	1.9177	1.1825	.8090	.2507	.1048
561	294149	2.3069	1.4529	1.0522	.2524	.1316
571	298149	2.2775	1.2765	.8873	.3046	.0688
581	303016	1.9000	.9333	.5203	.1316	.2618
591	308745	1.8129	1.0078	.6102	.2619	.1180
601	314063	2.1436	1.3303	.8099	.1571	.3444
611	318218	2.6787	1.6683	1.2631	.3718	.0181
621	321607	3.1082	1.9429	1.4079	.4423	.0735

Sample Depth (cm)	Age (yrs.)	cm/1000 yrs	Total Rate	Carbonate	Opal	"Detritus"
631	324669	3.2689	1.8424	1.3220	.4072	.0983
641	327726	3.1491	1.9206	1.3085	.5043	.0884
651	331030	2.8801	1.6201	1.1098	.4162	.0784
661	334688	3.1200	1.6071	.9416	.3728	.2696
671	337540	4.1845	2.4057	1.5437	.2525	.5985
681	339596	3.6496	2.3168	1.7068	.1246	.4686
691	343701	2.0975	1.3879	.9762	.2202	.1710
701	349387	1.8548	1.2774	.9427	.2054	.1105
713	355538	2.2009	1.5320	1.1734	.2661	.0754
721	358802	2.5051	1.7623	1.3461	.3098	.0902
731	362709	2.4193	1.5607	1.1153	.3664	.0616
741	367097	2.1968	1.2990	.8904	.3229	.0677
751	371826	2.2192	1.2831	.8860	.3181	.0605
761	376129	2.8471	1.6089	1.0995	.4008	.0896
771	379096	3.6171	1.9388	1.3798	.3116	.2339
781	381684	4.5099	2.2865	1.5873	.5304	.1446
791	383624	4.7690	2.2934	1.5730	.0393	.6743
801	385906	3.7413	1.8718	1.0896	.4751	.2825
811	389131	3.4526	1.6790	1.0837	.3301	.2488
821	391760	3.3032	1.5604	1.0729	.3255	.1473
831	395329	2.4713	1.5572	1.1005	.2932	.1436
841	400000	2.1030	1.4803	1.0764	.3354	.0510
851	404842	2.0307	1.4954	1.0612	.1937	.2230
861	409851	1.9417	1.4932	1.1230	.1435	.2093
871	415151	1.8316	1.4059	1.0328	.2692	.0862
881	420781	1.8309	1.4030	1.0763	.2434	.0648
891	426084	2.0488	1.5759	1.2483	.2511	.0590
901	430605	2.6468	2.0436	1.6009	.2642	.1591
911	433850	3.6879	2.7154	2.0005	.2593	.4408
921	436179	3.8970	2.7295	2.0324	.4026	.2783
931	439036	3.2078	2.2272	1.6482	.2585	.3016
946	444181	2.6212	1.8039	1.4124	.3115	.0639
951	446329	2.1548	1.3780	.9893	.3166	.0529

Accumulation Rates for Y69-73P

Sample Depth (cm)	Age (yrs.)	cm/1000 yrs.	Total Rate	Carbonate	Opal	"Detritus"
20	6136	7.9610	4.5060	3.3660	.4040	.7140
30	7392	10.5940	5.9960	4.4970	.5040	.9730
40	8148	13.2970	7.5260	5.3740	.7930	1.3320
50	8900	12.5100	7.0810	4.8360	.7130	1.5010
60	9753	11.4540	6.4830	4.4340	.7180	1.3000
70	10647	9.5800	5.4220	4.0290	.2870	1.0810
80	11901	7.2980	4.1310	3.1680	.3300	.5980
90	13411	7.2630	4.1110	3.1900	.2170	.6730
100	14676	8.6560	4.8990	3.8460	.3550	.6700
110	15739	9.3470	5.2900	3.9680	.4780	.8170
120	16815	9.2500	5.2350	3.8380	.5360	.8300
130	17900	11.7300	6.6390	4.8000	.6130	1.1900
140	18602	16.2130	9.1770	6.9100	.3060	1.9430
150	19152	14.9660	8.4710	6.1410	.5410	1.7560
160	20003	11.2280	6.3550	4.6710	.5870	1.0640
170	20937	11.9750	6.7780	4.6970	.7050	1.3440
180	21692	11.1890	6.3330	4.7050	.5200	1.0870
190	22789	8.8170	4.9900	3.5080	.5430	.8980
200	23955	8.8090	4.9860	3.5500	.3970	1.0180